Modelling of wine vinegar acetification bioreactor: global sensitivity analysis and simplification of the model

Jorge E. Jiménez-Hornero [a*], Inés Mª Santos Dueñas [b] and Isidoro García-García [b]

[a] Department of Electrical Engineering and Automatic Control, University of Cordoba, Campus Rabanales, 14071 Cordoba, Spain

[b] Department of Chemical Engineering, University of Cordoba, Campus Rabanales, 14071 Cordoba, Spain

[*] Correspondence: jjimenez@uco.es; Tel.: +34-957-212-079

Abstract

First-principles models of any process usually describe its complex underlying mechanisms using differential and algebraic equations including several unknown parameters, whose values must be normally estimated from experimental data. In this context, assessment of the influence of each parameter on model outputs, also known as sensitivity analysis, is an invaluable tool to, for example, simplify the structure of such model. In this work, variance-based Global Sensitivity Analysis (GSA) using Sobol' main and total effects was carried out on a previously proposed acetification process first-principles model. Three parameters (K_{SE}, K_{IA} and K_{SO}) showed less influence than the remaining nine considering their stated value ranges; K_{SE} presented no influence in all the analysed experimental conditions, value variation of K_{IA} exhibited a slightly greater effect on experiments with higher mean acetic acid concentrations and K_{SO} showed the strongest impact by varying its value in all the experiments. According to these results, the model was simplified and its simulation compared with the initially proposed model and the experimental data. The analysis performed, by way of example, can be of crucial importance for any other process.

Keywords

Sensitivity analysis; Bioprocess modelling; Model validation; Bioreactor systems; Acetification; Vinegar

1 Introduction

The design, analysis and optimization of any process are fundamental stages to ensure that any process in which we are interested can be a success in the context of an increasingly competitive world and in which multiple restrictions must be taken into account: economic, social, use of material and energy resources, waste reduction, etc. To achieve the above objectives, the modelling of the processes is a task of enormous importance, since it allows proposals to be made that represent the complex interactions between all the variables that must be considered and, in this way, carry out an analysis and optimization of which should be the operational conditions to be used.

Mathematical models are invaluable tools in many fields of science and engineering [1–3] where, independently of their type (first-principles models, black-box models, etc.), they are used for a broad range of applications like evaluating scenarios, explore cause-effect relations, decision-making, etc [4]. Although the modelling of any process is a difficult task, when working with bioprocesses, the complexity is usually very high; biotechnological processes involve complex mechanisms which are usually translated into models typically oriented to make predictions or to optimize their performance with objective functions like productivity, reaction rates, etc [5]. For any type of process, when first-principles models are used, they include proposed algebraic kinetic equations with a certain number of associated parameters, along with ordinary or partial differential equations corresponding to mass and energy balances [6]. This makes necessary to estimate these parameters from experimental data, a difficult task considering the related drawbacks that can appear, like identifiability problems, estimation precision [3,7,8], etc. Therefore, it is advisable, among other aspects, to propose models that are as simplified as possible, as well as the use of robust procedures for evaluating the sensitivity of the parameters on the response of the models.

Then, an important task is the sensitivity analysis (SA) which allows to assess the influence of the change of the value of the parameters on the model outputs [9]. Additionally, among other purposes [6], it can be used for dimensionality reduction of models through the determination of uninfluential parameters and, therefore, helping to simplify them. Reviews about both theory and application fields of SA can be found in [4,10–13]. In general, SA methods can be classified into two groups: Local Sensitivity Analysis

(LSA) or Global Sensitivity Analysis (GSA) [5,14,15]. LSA investigates how a small change on the value of each parameter affects the model outputs, being these changes calculated by gradients or partial differentiation on a particular point in the parameter space, so its main shortcoming is that analysis results are only valid around such point. On the other hand, GSA explores all the parameter space along with parameter interaction effects, something particularly important in nonlinear models (which it is frequently the case when working with biological processes). Among the different approaches to carry out GSA [6], one of the most common is the variance-based or Sobol' method [16,17], which analyses the contribution of individual parameters or groups of them to the outputs variance.

An interesting example of biotechnological process, well studied by the authors, is the wine vinegar production, where a strictly aerobic group of microorganisms, acetic acid bacteria, oxidize ethanol into acetic acid [18]. Among other modelling approaches [19], a first-principles model was proposed by the authors in a previous work [20], which is nonlinear with respect to its parameters and with known identifiability issues [7]. In the scope of parameter estimation, a procedure involving LSA was implemented to identify the most influential parameters [8]; this procedure, although complex, allowed obtaining a model with a good fit to experimental data. Now, the novelty and intended objective of this work is twofold: 1) to broaden the sensitivity analysis using GSA for screening all the parameter space, not only local points, and to reassess influences on model outputs; GSA is an interesting general methodology for analysing parameter-output cause-effect relations as well as for model reduction 2) to simplify, if possible, the initial model maintaining the same validity domain using results from GSA.

2 Experimental

2.1 Raw material and microorganisms

White wine from the Montilla-Moriles D.O. (Córdoba, Spain) containing (11.7 ± 0.3) % (v/v) ethanol and an initial acidity of (0.4 ± 0.1) % (w/v) as acetic acid was used as substrate.

The inoculum was a natural mixed culture of Acetic Acid Bacteria (AAB) which, as usual in vinegar industry, was obtained from acetators carrying out several repeated acetification cycles using the same substrate.

2.2 Experimental set-up

Experiments were conducted using an 8 L acetator from Heinrich Frings GmBH & Co. KG (Rheinbach, Germany) equipped with a self-aspirating turbine to get a high oxygen transfer efficiency between the inlet gas and the substrate [21]. Several sensors and actuators were added to the equipment along with a FieldPoint I/O system and a LabView (National Instruments Corp., Austin, USA) computer program to get an automated operation, as described in detailed in [20,22–25]. This arrangement allowed the unattended bioreactor loading and unloading as well as the process monitoring, resulting in highly reproducible cycles and efficient control and data logging of key variables. The setup was completed with a condenser to minimize volatile losses, so an acetic acid yield on ethanol of at least 95% of the theoretical one was obtained in all the experiments.

2.3 Analytical methods

Acidity was determined by acid-base titration with an NaOH solution approximately 0.5 N that was previously standardized with potassium hydrogen phthalate. Ethanol concentration and volume were both online measured using an Alkosens probe with an Acetomat transducer from Heinrich Frings GmbH & Co. KG (Rheinbach, Germany) and an EJA 110 differential pressure probe from Yokogawa Electric Corp. (Tokyo, Japan), respectively. Also, viable and total cell concentrations were obtained by using the counting method described in [26]; non-viable cell concentrations are determined subtracting viable cell concentrations to total cell ones.

2.4 Experimental conditions

Different experiments were conducted according to a semi-continuous operation mode near to industrial conditions, in which the acetification process was developed until ethanol was depleted to a desired extent. Once such predetermined ethanol concentration was reached, a percentage of the bioreactor volume was unloaded and, after that, the tank was slowly loaded following a continuous or semi-continuous mode with fresh raw material until the working volume (8 L) was achieved (see Section S1 in supplementary material for a detailed description).

The experiments used along with the values of their operational variables are summarized in Table 1 and they are defined to cover a broad range of process conditions. All the experiments were carried out at a constant temperature of 31 ºC and with a constant input air flow rate of 7.5 L air·h^{-1}·L^{-1} medium. Initial waste cycles were carried out until a repetitive experimental behaviour was achieved and, after that, several production cycles (at least ten) were developed at each condition. Obtained results for each experiment, which have been previously published elsewhere [8,19], are described in Section S2 of supplementary material; they have been included again because a new discussion is carried out on them in this work (they have been used for GSA of the proposed model).

Table 1. Experiments used for parameter estimation of the proposed model. E_{max} is the maximum ethanol concentration allowed during semi-continuous loading mode (*% v/v*); E_{unload} is the ethanol concentration at the end of the cycle (*% v/v*); $V_{unloaded}$ is the percentage of unloaded volume (*%*) and F_i is the loading flow rate ($L \cdot min^{-1}$)

Experiment	Loading mode	E_{max}	E_{unload}	$V_{unloaded}$	F_i
1	Continuous	-	2	75	0.035
2	Continuous	-	2	50	0.035
3	Continuous	-	2	25	0.035
4	Continuous	-	3.5	50	0.035
5	Continuous	-	0.5	50	0.035
6	Continuous	-	0.5	75	0.01
7	Continuous	-	3.5	25	0.06
8	Semi-continuous	5	1.5	50	0.02
9	Semi-continuous	5	0.5	50	0.02

2.5 Mathematical model

Proposed first-principles model for the acetification process, used in the present work, was described in [20,22] and is stated in equations (1)-(21). Mass balances (equations (1)-(6)) and kinetic equations (equations (7)-(21)) were included, but no energy balance equations, because all the experiments were developed at isothermal conditions.

$$V\frac{dX_v}{dt} + X_v\frac{dV}{dt} = V\left(r_{X_c} - r_{X_d}\right) \quad (1)$$

$$V\frac{dX_d}{dt} + X_d\frac{dV}{dt} = V\left(r_{X_d} - r_{lysis}\right) \quad (2)$$

$$V\frac{dE}{dt} + E\frac{dV}{dt} = F_i \cdot E_0 - V \cdot r_E \quad (3)$$

$$V\frac{dA}{dt} + A\frac{dV}{dt} = V \cdot r_A \quad (4)$$

$$V\frac{dO}{dt} + O\frac{dV}{dt} = F_i \cdot O^0 + V[\beta(O^0 - O) - r_{OE}] \quad (5)$$

$$\frac{dV}{dt} = F_i \quad (6)$$

$$r_{X_c} = \mu_c \cdot X_v \quad (7)$$

$$\mu_c = \mu_{max} \cdot f_e \cdot f_a \cdot f_o \quad (8)$$

$$f_e = \frac{E}{E + K_{SE} + \frac{E^2}{K_{IE}}} \quad (9)$$

$$f_a = \frac{1}{1 + \left(\frac{A}{K_{IA}}\right)^4} \quad (10)$$

$$f_o = \frac{O}{O + K_{SO}} \quad (11)$$

$$r_{X_d} = \mu_d \cdot X_v \quad (12)$$

$$\mu_d = \mu_d^0 \cdot f_{dE} \cdot f_{dA} \quad (13)$$

$$f_{dE} = 1 + \left(\frac{E}{K_{mE}}\right)^4 \quad (14)$$

$$f_{dA} = 1 + \left(\frac{A}{K_{mA}}\right)^4 \quad (15)$$

$$r_{lysis} = \mu_{lysis} \cdot X_d \quad (16)$$

$$r_E = a_{E/X} \cdot r_{X_c} \quad (17)$$

$$r_A = \frac{r_E}{Y_{\frac{E}{A}}} \quad (18)$$

$$r_{OE} = \frac{r_E}{Y_{\frac{E}{O}}} \quad (19)$$

$$\beta = \frac{K_L a}{1 + \frac{K_L a}{VV_m} \cdot \frac{RT}{H}} \quad (20)$$

$$VV_m = \frac{Q}{V} \quad (21)$$

where:

- t is the time (h).
- X_v, X_d, E, A and O are the concentrations (g·L^{-1}) of viable cells, dead cells, ethanol, acetic acid and dissolved oxygen, respectively.
- V is the volume of the medium (L), F_i is the raw material feed rate (L·h^{-1}), E_0 is its ethanol concentration (g·L^{-1}) and Q is the air feed rate (L·h^{-1}).
- r_{X_c} is the cell growth rate, r_{X_d} is the cell death rate and r_{lysis} is the cell lysis rate (all in g·L^{-1}·h^{-1}).
- r_E is the ethanol uptake rate, r_A is the acetic acid formation rate and r_O is the dissolved oxygen uptake rate (all in g·L^{-1}·h^{-1}).
- μ_c is the specific growth rate (h^{-1}) and f_e, f_a and f_o are terms representing the influence of ethanol, acetic acid and dissolved oxygen on cell growth, respectively.
- μ_d is the specific cell death rate (h^{-1}) and f_{dE} and f_{dA} are terms representing the influence of ethanol and acetic acid on cell death, respectively.
- O^0 is the dissolved oxygen in equilibrium with air (0.076 g·L^{-1}), $a_{E/X}$ is the ethanol yield factor required to supply the amount of energy needed for biomass growth (experimentally obtained as 116.96 g ethanol·g^{-1} cell), $Y_{E/A}$ is the stoichiometric coefficient of ethanol uptake for acetic acid formation (0.767 g ethanol·g^{-1} acetic acid) and $Y_{E/O}$ is the stoichiometric coefficient of ethanol relative to oxygen (1.44 g ethanol·g^{-1} oxygen).
- β is a constant covering the following terms: $K_L a$ is the overall volumetric coefficient of mass transfer for the liquid phase (experimentally determined as 500 h^{-1}), VV_m is the ratio of the air feed rate to the volume of the medium (h^{-1}), R is the universal gas constant (0.082 atm·L·K^{-1}·mol^{-1}), T is the temperature (K) and H is the Henry's constant (atm·L·mol^{-1}).

The included model parameters were: μ_{max} (maximum value of μ_c, h^{-1}), K_{SE} (ethanol saturation constant, g ethanol·L^{-1}), K_{IE} (ethanol inhibition constant, g ethanol·L^{-1}), K_{IA} (acetic acid inhibition constant, g acetic

acid·L^{-1}), K_{SO} (dissolved oxygen saturation constant, g oxygen·L^{-1}), μ_d^0 (minimum value of μ_d, h^{-1}), K_{mE} (ethanol-induced cell death rate constant, g·L^{-1}), K_{mA} (acetic acid-induced cell death rate constant, g·L^{-1}) and μ_{lysis} (specific cell lysis rate, h^{-1}). These parameters were estimated using data from the experiments in Table 1 [8], obtaining the values shown in Table 2.

Table 2. Estimated model parameters [8]

Parameter	Estimated value
μ_{max}	0.614 h^{-1}
K_{SE}	3.73 g ethanol·L^{-1}
K_{IE}	10.9 g ethanol·L^{-1}
K_{IA}	100.14 g acetic acid·L^{-1}
K_{SO}	3.28 × 10^{-4} g oxygen·L^{-1}
μ_d^0	2.56 × 10^{-5} h^{-1}
K_{mE}	37.63 g ethanol·L^{-1}
K_{mA}	12.69 g acetic acid·L^{-1}
μ_{lysis}	0.48 h^{-1}

2.6 Global sensitivity analysis

The method used for global sensitivity analysis was a widely used variance-based one [27–29] through Sobol's sensitivity indices [16,30]. The total variance D of a model output $Y = f(X_1, X_2, \dots, X_k)$ is decomposed into a sum of 2^k partial variance terms corresponding to combinations of model parameters $X_1, X_2, \dots, X_k$ in increasing dimensionality (22) [14].

$$D = \int_{\Omega_k} f^2(x)dx - f_o^2 = \sum_{i=1}^{k} D_i + \sum_{1 \le i < j \le k} D_{ij} + \cdots + D_{1,2,\dots,k} \quad (22)$$

where Ω_k is the multidimensional parameter space, $f_0 = \int_{\Omega_k} f(x)dx$ and $D_{i_1,\dots,i_m}$ $(1 \le i_1 < \cdots < i_m \le k)$ represents the terms in the right-hand side, being the variance contribution of parameter combination $\{i_1, i_2, \dots, i_m\}$ [16], which is calculated by multiple integration [29]; in particular, $D_i = V_{X_i}\left(E_{X_{\sim i}}(Y|X_i)\right)$, where X_i is the i-th parameter and $X_{\sim i}$ is the set of all parameters but X_i, i.e., the inner expectation represents the mean value of Y considering all possible values of $X_{\sim i}$ while keeping X_i fixed and the outer variance is calculated considering all possible values of X_i.

Dividing (22) by total variance D results in equation (23)

$$\sum_{i=1}^{k} S_i + \sum_{1 \le i < j \le k} S_{ij} + \cdots + S_{1,2,\dots,k} = 1 \tag{23}$$

where $S_i = \frac{V_{X_i}\left(E_{X_{\sim i}}(Y|X_i)\right)}{D}$ is called the first-order sensitivity index or main effect of parameter i and represents the fraction of the total variance attributed to the uncertainty of each X_i alone. Another important variance-based measure is the total-order sensitivity index or total effect of parameter i, $S_{Ti} = 1 - \frac{V_{X_{\sim i}}\left(E_{X_i}(Y|X_{\sim i})\right)}{D}$ [31], which represents the contribution to the total variance of all higher-order (interaction) terms of (23) in which X_i is involved. If the model is additive, i.e., without parameter interactions, then all $S_{Ti} = 0$ and $\sum_{i=1}^{k} S_i = 1$. In conjunction, S_i and S_{Ti} are suitable measures of the global sensitivity of a given model output with respect to the model parameters.

In practice, S_i and S_{Ti} are estimated by sampling the parameter space using two independent matrices A_{nxk} and B_{nxk} (24), where n is the number of samples, and performing model simulations. Different parameter sampling strategies can be used, as uniform distributions or quasi-random sequences [32].

$$A = \begin{bmatrix} X_{11} & \cdots & X_{1k} \\ \vdots & \ddots & \vdots \\ X_{n1} & \cdots & X_{nk} \end{bmatrix}_{nxk} \qquad B = \begin{bmatrix} X'_{11} & \cdots & X'_{1k} \\ \vdots & \ddots & \vdots \\ X'_{n1} & \cdots & X'_{nk} \end{bmatrix}_{nxk} \tag{24}$$

Additional matrices A_B^i (25) are also necessary, whose columns are from A except the ith one, which is from B.

$$A_B^i = \begin{bmatrix} X_{11} & \dots & X'_{1i} & \dots & X_{1k} \\ X_{21} & \dots & X'_{2i} & \dots & X_{2k} \\ \dots & \dots & \dots & \dots & \dots \\ X_{n1} & \dots & X'_{ni} & \dots & X_{nk} \end{bmatrix} \quad (25)$$

Estimators for S_i and S_{Ti} can be obtained according to equations (26)-(27) [29] from matrices in (24)-(25).

$$\hat{S}_i = \frac{\frac{1}{n}\sum_{j=1}^{n} f(B)_j \left[f\left(A_B^i\right)_j - f(A)_j \right]}{D} \quad (26)$$

$$\hat{S}_{Ti} = \frac{\frac{1}{2n}\sum_{j=1}^{n} \left(f(A)_j - f\left(A_B^i\right)_j \right)^2}{D} \quad (27)$$

Estimation of total variance D can be obtained from equations (28).

$$f_0 = \frac{1}{n}\sum_{j=1}^{n} f(A)_j \qquad D = \frac{1}{n}\sum_{j=1}^{n} f^2(A)_j - f_0^2 \quad (28)$$

3 Results and discussion

Sobol' sensitivity indices of each parameter (main effects and total effects) have been calculated to carry out the GSA on several outputs of the acetification process model, stated in Section 2.5, to quantify the influences or effects of such parameters. Outputs considered are viable and non-viable cell concentrations (X_v and X_d), ethanol concentration (E) and acetic acid concentration (A); dissolved oxygen concentration (O) has not been used in the analysis because the low tension superficial of the medium as well as the aeration mode of this type of bioreactor lead to significant uncertainties regarding the measures of the dissolved oxygen concentration in the liquid phase, as discussed in [8], [21] and [22].

Experiments 1-6 from Table 1 were used for the GSA, intending to cover a broad range of operating conditions. Although a more detailed discussion has been previously carried out in [8], by way of summary, it can be indicated that to establish the range of variation of the parameters, it has been taken into account, among other aspects, the physical significance of each parameter, the maximum and minimum values of ethanol and acetic acid concentrations that can be found in the most common operating conditions, as well as typical values found in the literature for similar kinetic parameters. Then,

model parameters are defined in Section 2.5 and their variation ranges are shown in Table 3. Such ranges were defined considering the following constraints [8]:

a) Parameters can only take positive values.

b) Parameter values leading to out-of-the-bounds values of kinetic functions were rejected.

c) Parameter values out of physical meaning were also rejected.

Table 3. Ranges of model parameters values

Parameter	Range
μ_{max}	[0,2] h^{-1}
K_{SE}	[0,10] g ethanol·L^{-1}
K_{IE}	[0.25,90] g ethanol·L^{-1}
K_{IA}	[80,120] g acetic acid·L^{-1}
K_{SO}	[0,1.5] × 10^{-3} g oxygen·L^{-1}
μ_d^0	[0,2] h^{-1}
K_{mE}	[10,90] g ethanol·L^{-1}
K_{mA}	[10,120] g acetic acid·L^{-1}
μ_{lysis}	[0,2] h^{-1}

Parameter ranges from Table 3 were sampled using the Sobol' method to obtain quasi-random low-discrepancy parameter vectors [33]. The main benefit of this method is that parameter samples are more uniformly and homogeneously distributed over the respective ranges, covering better the parameter space. In this work, 5000 parameter vectors (samples) were generated using this method. On the other hand, model numerical integration was done with a variable-step variable-order solver for Differential-Algebraic Equations (DAEs) based on Numerical Differentiation Formulas (NDFs) and included in MATLAB (Mathworks Inc., Natick, USA).

Estimators of main effects ($\hat{S}_i$) and total effects ($\hat{S}_{Ti}$) of each parameter were calculated using equations (26)-(27). Time courses of both estimators on each considered output for Experiment 1 are shown in Figures 1-4.

Figure 1

Figure 2

Figure 3

Figure 4

At a first glance, main and total effects of parameters K_{SE} and K_{IA} show very low values during all simulation time on all outputs, and μ_{lysis} only exhibits (strong) influence on X_d, but it is difficult to quantify the influence of the remaining parameters. For a better assessment of $\hat{S}_i$ and $\hat{S}_{Ti}$, the areas under their time course curves from Figures 1-4 are calculated to estimate the accumulated influence of every parameter on each output over all simulation time. These areas are comparatively shown in Figure 5.

Figure 5

As previously suggested, K_{SE} and K_{IA} exhibit a negligible influence over all outputs, considering the operational conditions of Experiment 1. On the other hand, parameters K_{mE}, K_{mA} and μ_d^0 show strong effects over all outputs, while μ_{max} and K_{IE} present lower influences on X_v and X_d , but strong ones on E and A; the influence of K_{SO} is low on X_v and X_d, but its total effect is noticeable on E and A. Interestingly, μ_{lysis} has no influence on any output except on X_d, where is very high. Furthermore, large differences can be observed comparing the main and total effects in almost all the parameters, which means strong interaction or joint effects among them. These results are in agreement with those in [8] regarding to parameters K_{SE}, K_{IA}, μ_{max}, μ_d^0 and μ_{lysis}, but differ with respect to K_{IE}, K_{SO}, K_{mE} and K_{mA};

these discrepancies might be expected considering that LSA was carried out in that previous work which, because of its own nature, doesn´t properly cover all the parametric space.

If the GSA is repeated using Experiments 2-6 (for analysis on broad experimental conditions), the achieved results are shown in Figures 6-10, where only the areas under $\hat{S}_i$ and $\hat{S}_{Ti}$ are considered to account for accumulated influences. On the other hand, mean acetic acid concentrations over time considering the ten cycles of all the experiments are shown in Table 4.

Figure 6

Figure 7

Figure 8

Figure 9

Figure 10

Table 4. Mean acetic acid concentrations for each experiment

Experiment	Mean acidity ($g \cdot L^{-1}$)
1	58.07
2	73.19
3	86.72
4	61.7
5	81.88
6	62.54
7	72.55
8	79.19
9	86.73

As can be observed, relative influences of the parameters are very similar in Experiments 2-6 to those obtained from Experiment 1, with little differences about which parameters show a higher effect with respect to the others. However, there are three parameters (K_{SE}, K_{IA} and K_{SO}) with lower influences than the remaining ones in all the experimental conditions.

Both main and total effects of K_{SE} are roughly null for all the experiments, so it is completely uninfluential on the considered model outputs without any joint or interactive effect with the remaining parameters; this means that K_{SE} could take any value within the analysed range (see Table 3), so that it can be assigned its lower value (0). Since K_{SE} is included as a summand in the denominator of equation (9) for f_e, this implies in practice that can be removed from the model, simplifying the expression for f_e to equation (30).

$$f_e = \frac{E}{E + \frac{E^2}{K_{IE}}} \tag{30}$$

Regarding to K_{IA}, it shows a negligible influence in Experiments 1, 4 and 6, but exhibits a low but noticeable effect on E and A outputs in Experiments 2, 3 and 5. The former are the experiments with lower mean acetic acid concentrations over the cycle while the latter are just those with higher ones (see Table 4), so the influence of K_{IA} is related with the acidity level in the medium. In fact, if equation (10) for f_a is analysed, it can be observed that, when the acetic acid concentration is low or medium, the term $\left(\frac{A}{K_{IA}}\right)^4$ can be neglected with respect to 1 (considering the variation range of K_{IA}, see Table 3) and $f_a \approx 1$ (i.e., noninfluential on μ_c) but, when the acetic acid concentration is relatively high, then $f_a < 1$ (particularly when K_{IA} has a low value) and, therefore, K_{IA} has certain effect on μ_c. Several simulations with values 80, 90, 110 and 120 g·L^{-1} for K_{IA} were done to check these statements, showing in figure 11 the time courses of ethanol concentration, by way of example, for all the experiments (including 7-9).

Figure 11

It can be observed that, if $K_{IA} \in [90,120]$ g·L^{-1}, the influence of its variation is low and that with $K_{IA} < 90$ g·L^{-1}, such influence is particularly marked on experiments with high mean acetic acid concentration (experiments 3, 5, 8 and 9); this agrees with the above analysis and allows to conclude that any value for $K_{IA} \in [90,120]$ g·L^{-1} would be appropriate for suitable model predictions. Therefore, the previously estimated value for K_{IA} (100.14 g acetic acid·L^{-1}) will be used.

K_{SO} shows, in general, higher main and total effects than K_{IA}, but they are relatively low compared with the influences of the other six parameters, so an analysis like the one done for K_{IA} will be carried out for K_{SO}. Simulations with values 0, 6·10^{-4}, 10·10^{-4} and 15·10^{-4} g oxygen·L^{-1} for K_{SO} were done and the resulting time courses of ethanol concentration for all the experiments are shown in Figure 12.

Figure 12

In this case, the variations in K_{SO} values have a stronger impact on the model outputs considering all the experiments (as can be seen from the GSA results, see Figures 5-10). Therefore, the non-influential interval for K_{SO} is narrower than for K_{IA} (presumably between 2.5·10^{-4} and 4.5·10^{-4} g oxygen·L^{-1}) and, consequently, the previously estimated value for K_{SO} (3.28·10^{-4} g oxygen·L^{-1}) will be also retained.

Since K_{SE} has no interactive effects with the other parameters and both K_{IA} and K_{SO} maintain their previously estimated values, it would not be necessary to re-estimate the other six parameters of the model.

To verify the goodness of the simplified model, time courses of all considered model outputs (viable cell, non-viable cell, ethanol and acetic acid concentrations) are shown, by way of example, in Figures 13-14, along with the ones from the initial model and the experimental data, for Experiments 1 and 9 in which the environmental conditions for the bacteria are very different, for example, the average acidity is 58 and 80 respectively ; results for all the experiments can be found in Section 3 of supplementary material).

As expected, K_{SE} removal had no impact on the outputs with respect to the initial model in all the analysed

experimental conditions.

Figure 13

Figure 14

4 Conclusions

Aiming to study the influence of its parameters in all their value ranges on model outputs, a global sensitivity analysis (GSA) using Sobol' indices was carried out on a previously obtained model for wine vinegar acetification process. Thus, a previous local sensitivity analysis (LSA) carried out by the authors was broadened, allowing screening all the parameter space and reassessing the initial model according to the obtained results, looking for its simplification. These objectives constitute the novelties of the work.

Main and total effects showed that parameters μ_{max}, K_{IE}, μ_d^0, K_{mE} and K_{mA} had the highest influences on all outputs considering the broad analysed operational conditions. The remaining parameters presented either low effects (K_{SE}, K_{IA} and K_{SO}) or only important influence on a certain output (it the case for μ_{lysis}, which only has effect, very strong indeed, on output X_d, so it must be retained). Some of these results are in agreement with those obtained in the previous work, but other not; the discrepancies show the limitations and drawbacks of LSA due to its local nature.

Model parameter concerning to growth limitation by ethanol (K_{SE}) could be removed from the model, since it had null main and total effects, but those related with growth inhibition by acetic acid (K_{IA}) and growth limitation by oxygen (K_{SO}) showed a narrower non-influential interval than their value ranges. In particular, the influence of K_{IA} depends on the acetic acid concentration present in the medium, but it can be considered that any value within the interval [90, 120] g acetic acid·L^{-1} would lead to results very close to those from the initial model. Regarding to K_{SO}, its variation affects the model outputs in all the experimental conditions, estimating the interval [2.5·10^{-4}, 4.5·10^{-4}] g oxygen·L^{-1} as non-influential. In both cases, retaining their previously estimated values was considered the most suitable option for these parameters.

Simulation results of the simplified model was compared with those from the initial one; the resultant outputs barely differ from those achieved in a previous work, validating the negligible influence of the

removed parameter in all the analysed experiments; therefore, suitable predictions in comparison with the experimental data can be also obtained from the simplified model.

Because of local sensitivity analysis (LSA) can only provide influence results around a single point in the parametric space, it is more advisable to perform a global sensitivity analysis (GSA), thus increasing the validity of the results obtained and, in particular, facilitating the analysis necessary to neglect certain parameters or reduce a model. This study is important for any type of chemical, biochemical or any other process in which the number of parameters involved in the proposed models is usually very high and, therefore, it is highly recommended to simplify them as much as possible.

Acknowledgements

This research was funded by "Junta de Andalucía. Convocatoria de subvenciones a proyectos de I+D+i universidades y entidades públicas de investigación (BOJA nº 119, de 23 de junio de 2020), Project P20_00590". "Programa PAIDI" from Junta de Andalucía (RNM-940).

Bibliography

[1] S.H. Baek, S.K. Jeon, K. Pagilla, J. Ind. Eng. Chem. 15(6) (2009) 835–40. 10.1016/j.jiec.2009.09.009.

[2] V.N. Sapunov, A.A. Stepacheva, E.M. Sulman, J. Wärnå, P. Mäki-Arvela, M.G. Sulman, A.I. Sidorov, B.D. Stein, D.Yu. Murzin, V.G. Matveeva, J. Ind. Eng. Chem. 46 (2017) 426–35. 10.1016/j.jiec.2016.11.013.

[3] D. Villanueva-Bermejo, T. Fornari, M.V. Calvo, J. Fontecha, J.A.P. Coelho, R.M. Filipe, R.P. Stateva, J. Ind. Eng. Chem. 82 (2020) 317–23. 10.1016/j.jiec.2019.10.029.

[4] A. Saltelli, K. Aleksankina, W. Becker, P. Fennell, F. Ferretti, N. Holst, S. Li, Q. Wu, Environ. Model. Softw. 114 (2019) 29–39. 10.1016/j.envsoft.2019.01.012.

[5] M. Tosin, A.M.A. Côrtes, A. Cunha, in: F. A. B. da Silva, N. Carels, M. Trindade dos Santos, F. J. P. Lopes (Eds.), Networks in Systems Biology: Applications for Disease Modeling, Springer International Publishing, Cham, 2020, pp. 93–118.

[6] S. Razavi, A. Jakeman, A. Saltelli, C. Prieur, B. Iooss, E. Borgonovo, E. Plischke, S. Lo Piano, T. Iwanaga, W. Becker, S. Tarantola, J.H.A. Guillaume, J. Jakeman, H. Gupta, N. Melillo, G. Rabitti, V. Chabridon, Q. Duan, X. Sun, S. Smith, R. Sheikholeslami, N. Hosseini, M. Asadzadeh, A. Puy, S. Kucherenko, H.R. Maier, Environ. Model. Softw. 137 (2021) 104954. 10.1016/j.envsoft.2020.104954.

[7] J.E. Jiménez-Hornero, I.M. Santos-Dueñas, I. García-García, Math. Biosci. 216(2) (2008) 154–62. 10.1016/j.mbs.2008.09.004.

[8] J.E. Jiménez-Hornero, I.M. Santos-Dueñas, I. García-García, Biochem. Eng. J. 45(1) (2009) 7–21. 10.1016/j.bej.2009.01.010.

[9] K. Konakli, B. Sudret, Reliab. Eng. Syst. Saf. 156 (2016) 64–83. 10.1016/j.ress.2016.07.012.

[10] J. Norton, Environ. Model. Softw. 69 (2015) 166–74. 10.1016/j.envsoft.2015.03.020.

[11] F. Pianosi, K. Beven, J. Freer, J.W. Hall, J. Rougier, D.B. Stephenson, T. Wagener, Environ. Model. Softw. 79 (2016) 214–32. 10.1016/j.envsoft.2016.02.008.

[12] E. Borgonovo, E. Plischke, Eur. J. Oper. Res. 248(3) (2016) 869–87. 10.1016/j.ejor.2015.06.032.

[13] H. Gupta, S. Razavi, in: G. P. Petropoulos, P. K. Srivastava (Eds.), Sensitivity Analysis in Earth Observation Modelling, Elsevier, 2017, pp. 397–415.

[14] Y. Zhang, A. Rundell, Syst. Biol. 153(4) (2006) 201–11. 10.1049/ip-syb:20050088.

[15] B. Sudret, Reliab. Eng. Syst. Saf. 93(7) (2008) 964–79. 10.1016/j.ress.2007.04.002.

[16] A. Saltelli, I.M. Sobol', Mat. Model. 7 (1995).

[17] I.M. Sobol', S. Kucherenko, Math. Comput. Simul. 79(10) (2009) 3009–17. 10.1016/j.matcom.2009.01.023.

[18] I. García-García, J.E. Jiménez-Hornero, I.M. Santos-Dueñas, Z. González-Granados, A.M. Cañete-Rodríguez, in: A. Bekatorou (Ed.), Advances in Vinegar Production, CRC Press, 2019, pp. 299–325.

[19] J.E. Jiménez-Hornero, I.M. Santos-Dueñas, I. García-García, Processes 8(7) (2020) 749. 10.3390/pr8070749.

[20] J.E. Jiménez-Hornero, I.M. Santos-Dueñas, I. García-García, Biochem. Eng. J. 45(1) (2009) 1–6. 10.1016/j.bej.2009.01.009.

[21] I. García-García, I.M. Santos-Dueñas, C. Jiménez-Ot, J.E. Jiménez-Hornero, J.L. Bonilla-Venceslada, in: L. Solieri, P. Giudici (Eds.), Vinegars of the World, Springer Milan, Milano, 2009, pp. 97–120.

[22] J.E. Jiménez-Hornero, Contribuciones al modelado y optimización del proceso de fermentación acética. PhD Thesis, Universidad Nacional de Educación a Distancia Madrid, Spain, 2007.

[23] I. García-García, D. Cantero-Moreno, C. Jiménez-Ot, S. Baena-Ruano, J. Jiménez-Hornero, I. Santos-Dueñas, J. Bonilla-Venceslada, F. Barja, J. Food Eng. 80(2) (2007) 460–4. 10.1016/j.jfoodeng.2006.05.028.

[24] S. Baena-Ruano, C. Jiménez-Ot, I.M. Santos-Dueñas, J.E. Jiménez-Hornero, J.L. Bonilla-Venceslada, C. Álvarez-Cáliz, I. García-García, J. Chem. Technol. Biotechnol. 85(7) (2010) 908–12. 10.1002/jctb.2368.

[25] I.M. Santos-Dueñas, J.E.J.- Hornero, A.M. Cañete-Rodriguez, I. Garcia-Garcia, Biochem. Eng. J. 99 (2015) 35–43. 10.1016/j.bej.2015.03.002.

[26] S. Baena-Ruano, C. Jiménez-Ot, I.M. Santos-Dueñas, D. Cantero-Moreno, F. Barja, I. García-García, Process Biochem. 41(5) (2006) 1160–4. 10.1016/j.procbio.2005.12.016.

[27] H. Christopher Frey, S.R. Patil, Risk Anal. 22(3) (2002) 553–78. 10.1111/0272-4332.00039.

[28] D.G. Cacuci, M. Ionescu-Bujor, Nucl. Sci. Eng. 147(3) (2004) 204–17. 10.13182/04-54CR.

[29] A. Saltelli, P. Annoni, I. Azzini, F. Campolongo, M. Ratto, S. Tarantola, Comput. Phys. Commun. 181(2) (2010) 259–70. 10.1016/j.cpc.2009.09.018.

[30] I.M. Sobol', Math. Comput. Simul. 55(1) (2001) 271–80. 10.1016/S0378-4754(00)00270-6.

[31] T. Homma, A. Saltelli, Reliab. Eng. Syst. Saf. 52(1) (1996) 1–17. 10.1016/0951-8320(96)00002-6.

[32] P. Bratley, B.L. Fox, ACM Trans. Math. Softw. 14(1) (1988) 88–100. 10.1145/42288.214372.

[33] I.M. Sobol, USSR Comput. Math. Math. Phys. 16(5) (1976) 236–42. 10.1016/0041-5553(76)90154-3.

Figure captions

Figure 1. Main and total effects $\hat{S}_i$, $\hat{S}_{Ti}$ on X_v (Experiment 1)

Figure 2. Main and total effects $\hat{S}_i$, $\hat{S}_{Ti}$ on X_d (Experiment 1)

Figure 3. Main and total effects $\hat{S}_i$, $\hat{S}_{Ti}$ on E (Experiment 1)

Figure 4. Main and total effects $\hat{S}_i$, $\hat{S}_{Ti}$ on A (Experiment 1)

Figure 5. Areas under $\hat{S}_i$ (blue) and $\hat{S}_{Ti}$ (red) on each output (Experiment 1)

Figure 6. Areas under $\hat{S}_i$ (blue) and $\hat{S}_{Ti}$ (red) on each output (Experiment 2)

Figure 7. Areas under $\hat{S}_i$ (blue) and $\hat{S}_{Ti}$ (red) on each output (Experiment 3)

Figure 8. Areas under $\hat{S}_i$ (blue) and $\hat{S}_{Ti}$ (red) on each output (Experiment 4)

Figure 9. Areas under $\hat{S}_i$ (blue) and $\hat{S}_{Ti}$ (red) on each output (Experiment 5)

Figure 10. Areas under $\hat{S}_i$ (blue) and $\hat{S}_{Ti}$ (red) on each output (Experiment 6)

Figure 11. Ethanol concentrations from model simulations using different K_{IA} values on all the experiments

Figure 12. Ethanol concentrations from model simulations using different K_{SO} values on all the experiments

Figure 13. Simulation of outputs from initial and simplified models (Experiment 1)

Figure 14. Simulation of outputs from initial and simplified models (Experiment 9)

Supplementary material

Modelling of wine vinegar acetification bioreactor: global sensitivity analysis and simplification of the model

Jorge E. Jiménez-Hornero [1*], Inés Mª Santos Dueñas[2] and Isidoro García-García [2]

[1] Department of Electrical Engineering and Automatic Control, University of Cordoba, Campus Rabanales, 14071 Cordoba, Spain

[2] Department of Chemical Engineering, University of Cordoba, Campus Rabanales, 14071 Cordoba, Spain

[*] Correspondence: jjimenez@uco.es; Tel.: +34-957-212-079

Supplementary information to Experimental section

S1. Description of the operating mode

As summarized in the main text, acetification experiments were conducted in a semi-continuous operation mode, where each cycle ends when a preset ethanol concentration is reached after its depletion; the bioreactor is then unloaded, leaving a certain residual volume of medium used as inoculum for the next cycle, which is started by slowly loading the tank with fresh raw material until the working volume is achieved (Figure S1). This operation mode prevents abrupt changes and excessively high concentrations of ethanol in the medium (Garcia-Garcia et al., 2009, 2019).

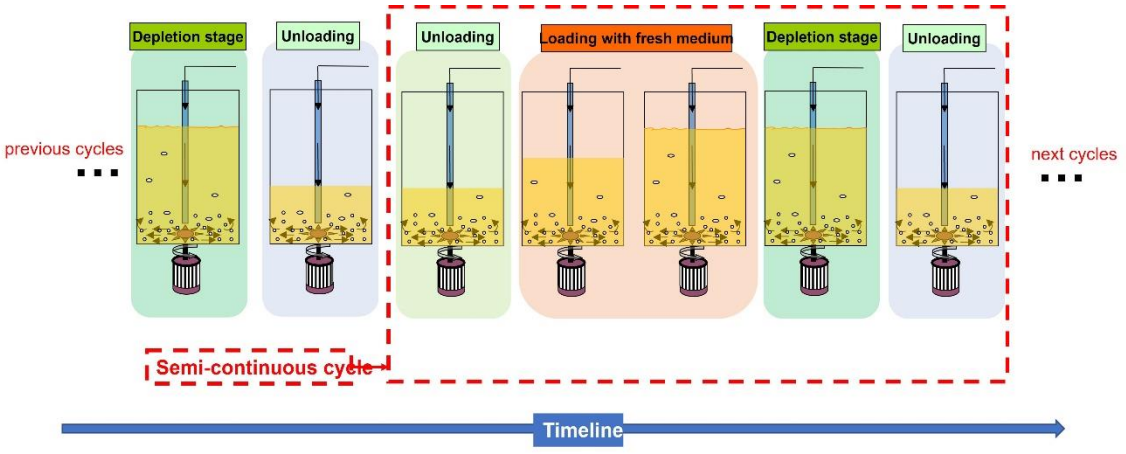

Figure S1. Semi-continuous operating mode for vinegar production

Typical used operational variables are the ethanol concentration at which the bioreactor is unloaded (E_{unload}), the unloaded volume of medium ($V_{unloaded}$), the loading mode and the raw material feeding flow rate (F_i) and the ethanol concentration in the fresh medium (E_0).

In practice, two different loading modes are used (see Table 1 in the main text):

- "Continuous": the bioreactor is slowly refilled without interruption until the working volume is achieved (Santos-Dueñas et al., 2015) (Figure S2).

- "Semi-continuous": the bioreactor is slowly refilled without exceeding a preset ethanol concentration E_{max} (Alvarez-Caliz et al., 2012) (Figure S3). In this case, loading is interrupted when the ethanol concentration in the medium is higher than the threshold value; loading is resumed when such concentration is again lower than the threshold. This refilling mode is repeated until the working volume is achieved.

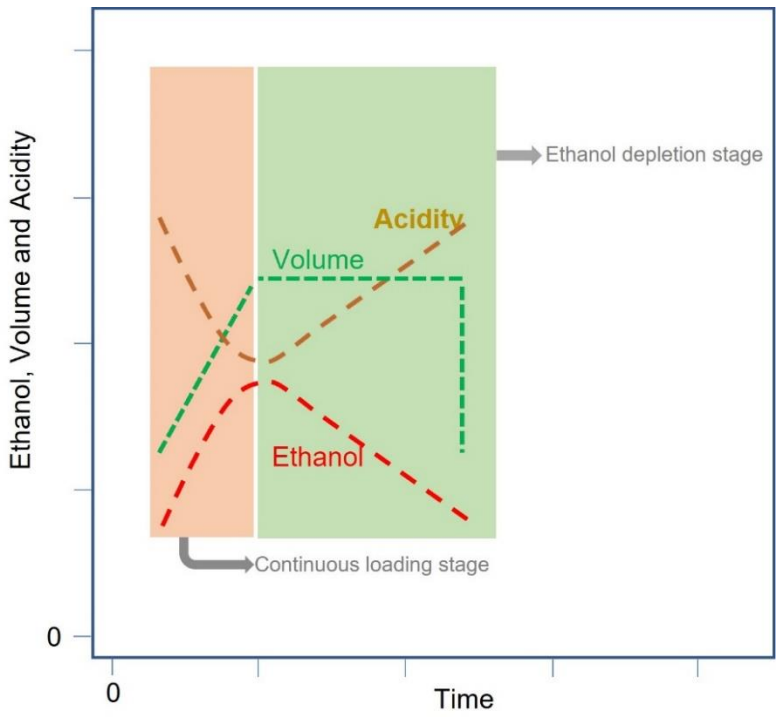

Figure S2. Continuous loading mode

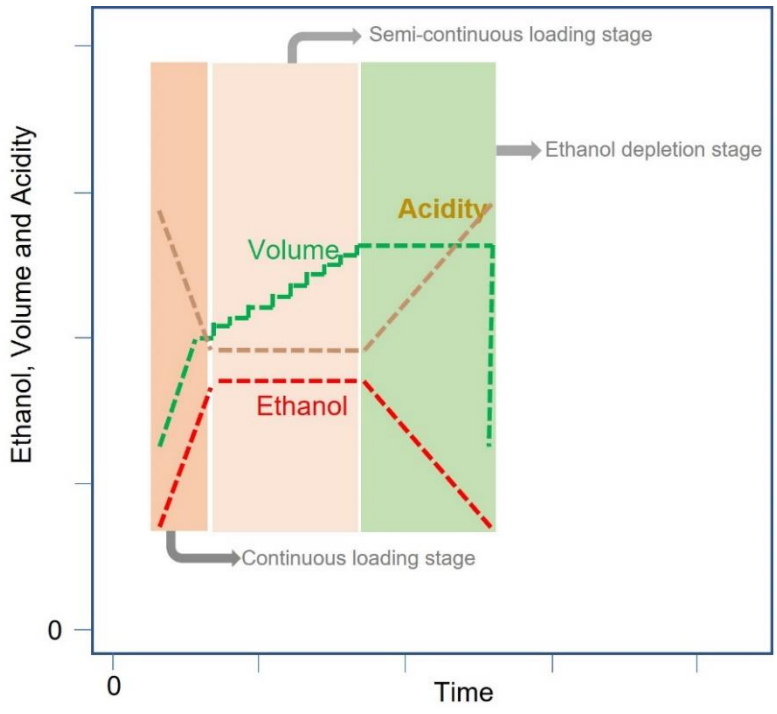

Figure S3. Semi-continuous loading mode

S2. Experimental conditions

In this section, all the experiments used in this work (see Table 1) will be described along with a summary of their main results.

Figure S4 shows viable cell (X_V), total cell (X), ethanol (E) and acetic acid (A) concentrations from ten cycles of Experiment 1, in which a continuous loading mode is used with E_{unload} = 2 % (v/v) (15.5 g·L^{-1}), $V_{unloaded}$ = 75 % and F_i = 0.035 L·min^{-1}.

Some results can be summarized as follows (mean ethanol uptake rate was calculated using the method described in (Garcia-Garcia et al., 2007) for all the experiments):

- Mean ethanol uptake rate: 1.6±0.1 g·L^{-1}·h^{-1}.
- Acetic acid production rate: 15.1±0.5 g·h^{-1}.
- Length of loading phase: 3.3±0.1 h.
- Total length of cycle: 37.5±1.1 h.
- Maximum ethanol concentration reached at the end of loading phase: 69±0.8 g·L^{-1}.
- Maximum acetic acid concentration at the end of the cycle: 95±1 g·L^{-1}.

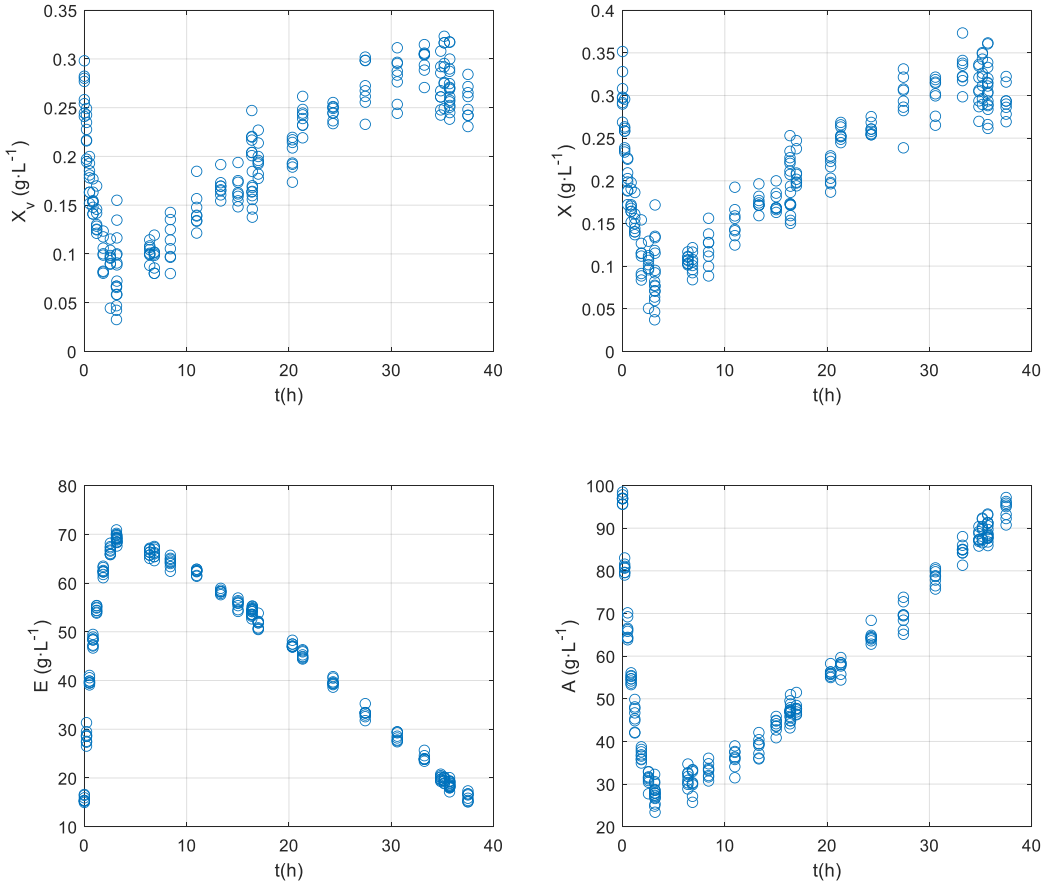

Figure S4. Time courses of the concentrations of the main variables from Experiment 1 (ten cycles)

Figure S5 shows viable cell (X_V), total cell (X), ethanol (E) and acetic acid (A) concentrations from ten cycles of Experiment 2, in which a continuous loading mode is used with E_{unload} = 2 % (v/v) (15.5 g·L^{-1}), $V_{unloaded}$ = 50 % and F_i = 0.035 L·min^{-1}.

Summary of main results:

- Mean ethanol uptake rate: 1.8±0.1 g·L^{-1}·h^{-1}.
- Acetic acid production rate: 17.1±0.5 g·h^{-1}.
- Length of loading phase: 1.8±0.1 h.
- Total length of cycle: 23±0.6 h.
- Maximum ethanol concentration reached at the end of loading phase: 48.8±0.8 g·L^{-1}.
- Maximum acetic acid concentration at the end of the cycle: 98±1 g·L^{-1}.

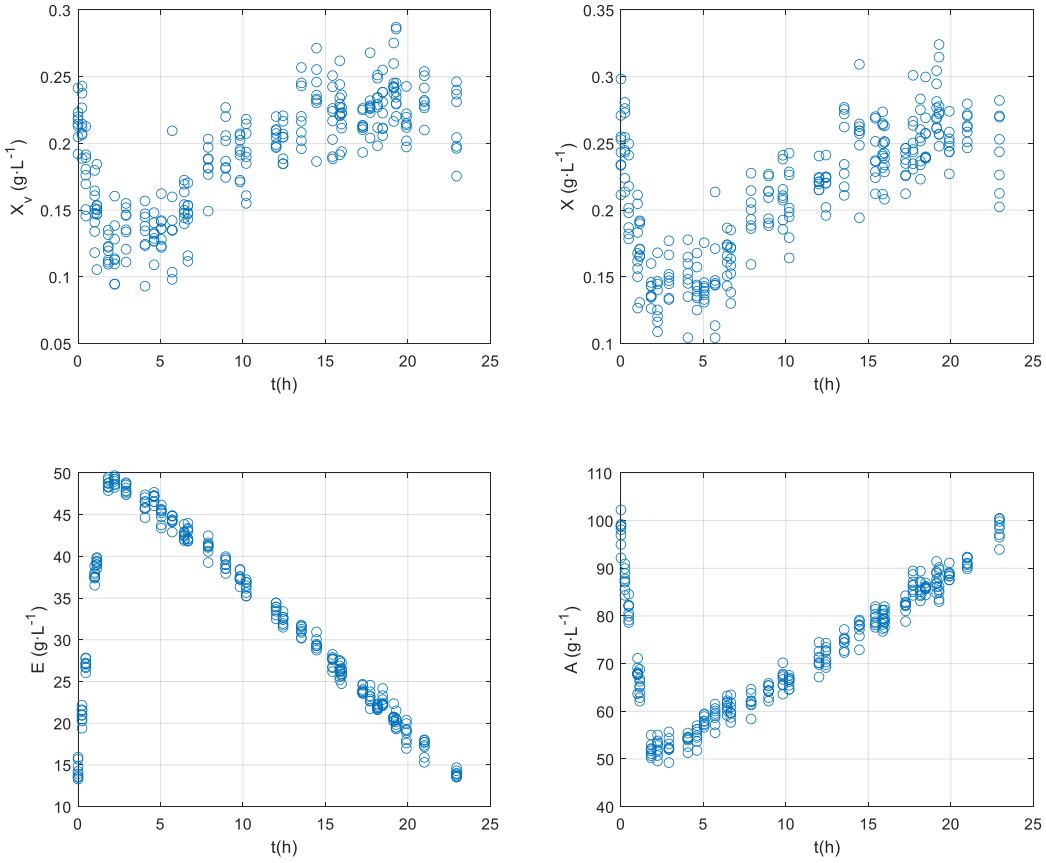

Figure S5. Time courses of the concentrations of the main variables from Experiment 2 (ten cycles)

Figure S6 shows viable cell (X_V), total cell (X), ethanol (E) and acetic acid (A) concentrations from ten cycles of Experiment 3, in which a continuous loading mode is used with E_{unload} = 2 % (v/v) (15.5 g·L^{-1}), $V_{unloaded}$ = 25 % and F_i = 0.035 L·min^{-1}.

Summary of main results:

- Mean ethanol uptake rate: 1.7±0.2 g·L^{-1}·h^{-1}.
- Acetic acid production rate: 17.3±0.4 g·h^{-1}.
- Length of loading phase: 0.9±0.1 h.
- Total length of cycle: 11.2±0.2 h.
- Maximum ethanol concentration reached at the end of loading phase: 31±0.8 g·L^{-1}.
- Maximum acetic acid concentration at the end of the cycle: 97±1 g·L^{-1}.

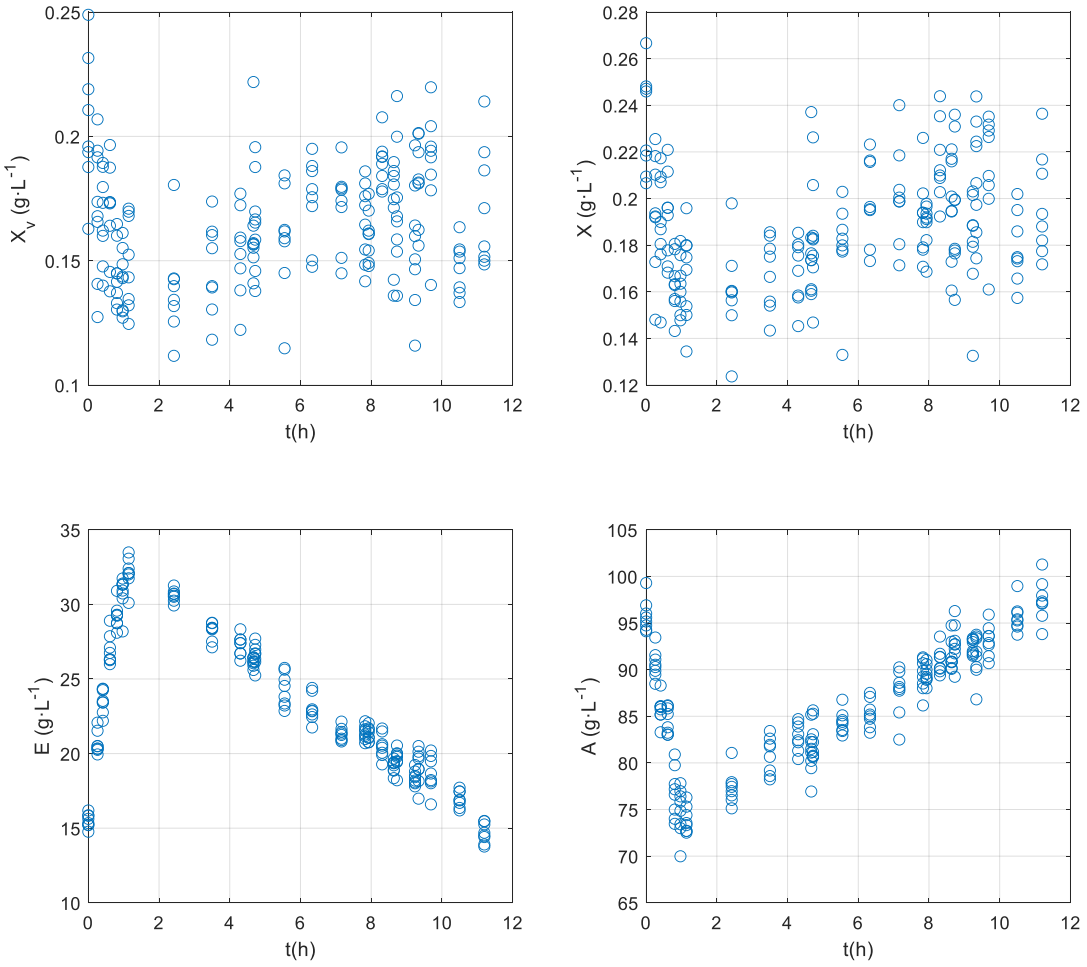

Figure S6. Time courses of the concentrations of the main variables from Experiment 3 (ten cycles)

Figure S7 shows viable cell (X_V), total cell (X), ethanol (E) and acetic acid (A) concentrations from ten cycles of Experiment 4, in which a continuous loading mode is used with E_{unload} = 3.5 % (v/v) (27.1 g·L^{-1}), $V_{unloaded}$ = 50 % and F_i = 0.035 L·min^{-1}.

Summary of main results:

- Mean ethanol uptake rate: 1.7±0.2 g·L^{-1}·h^{-1}.
- Acetic acid production rate: 16.3±0.4 g·h^{-1}.
- Length of loading phase: 2±0.1 h.
- Total length of cycle: 19.2±0.4 h.
- Maximum ethanol concentration reached at the end of loading phase: 55±0.8 g·L^{-1}.
- Maximum acetic acid concentration at the end of the cycle: 78±5 g·L^{-1}.

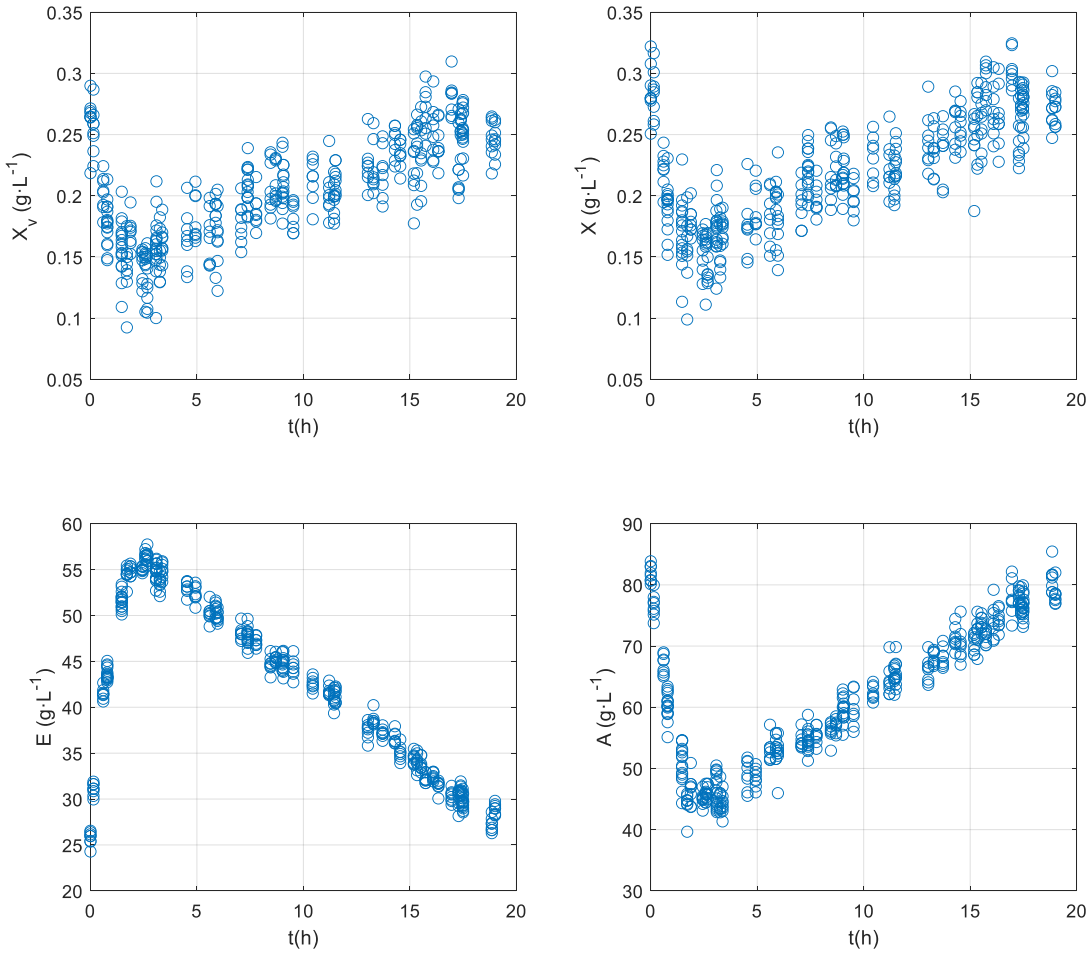

Figure S7. Time courses of the concentrations of the main variables from Experiment 4 (ten cycles)

Figure S8 shows viable cell (X_V), total cell (X), ethanol (E) and acetic acid (A) concentrations from ten cycles of Experiment 5, in which a continuous loading mode is used with E_{unload} = 0.5 % (v/v) (3.9 g·L^{-1}), $V_{unloaded}$ = 50 % and F_i = 0.035 L·min^{-1}.

Summary of main results:

- Mean ethanol uptake rate: 1.7±0.5 g·L^{-1}·h^{-1}.
- Acetic acid production rate: 14.7±0.3 g·h^{-1}.
- Length of loading phase: 2.1±0.1 h.
- Total length of cycle: 30±0.3 h.
- Maximum ethanol concentration reached at the end of loading phase: 45.7±0.8 g·L^{-1}.
- Maximum acetic acid concentration at the end of the cycle: 111±1 g·L^{-1}.

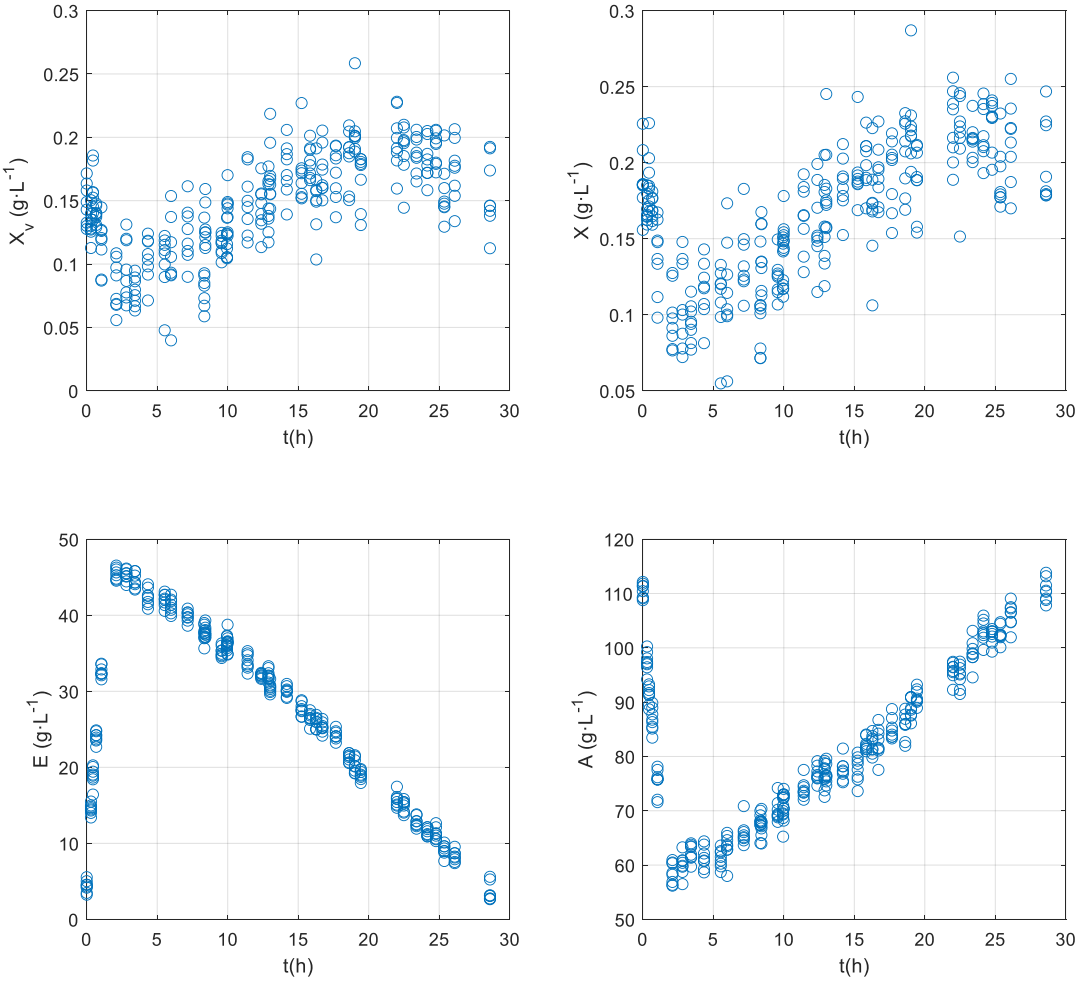

Figure S8. Time courses of the concentrations of the main variables from Experiment 5 (ten cycles)

Figure S9 shows viable cell (X_V), total cell (X), ethanol (E) and acetic acid (A) concentrations from ten cycles of Experiment 6, in which a continuous loading mode is used with E_{unload} = 0.5 % (v/v) (3.9 g·L^{-1}), $V_{unloaded}$ = 75 % and F_i = 0.01 L·min^{-1}.

Summary of main results:

- Mean ethanol uptake rate: 1.5±0.1 g·L^{-1}·h^{-1}.
- Acetic acid production rate: 14.3±0.3 g·h^{-1}.
- Length of loading phase: 9.6±0.1 h.
- Total length of cycle: 46±0.9 h.
- Maximum ethanol concentration reached at the end of loading phase: 62±0.8 g·L^{-1}.
- Maximum acetic acid concentration at the end of the cycle: 110±1 g·L^{-1}.

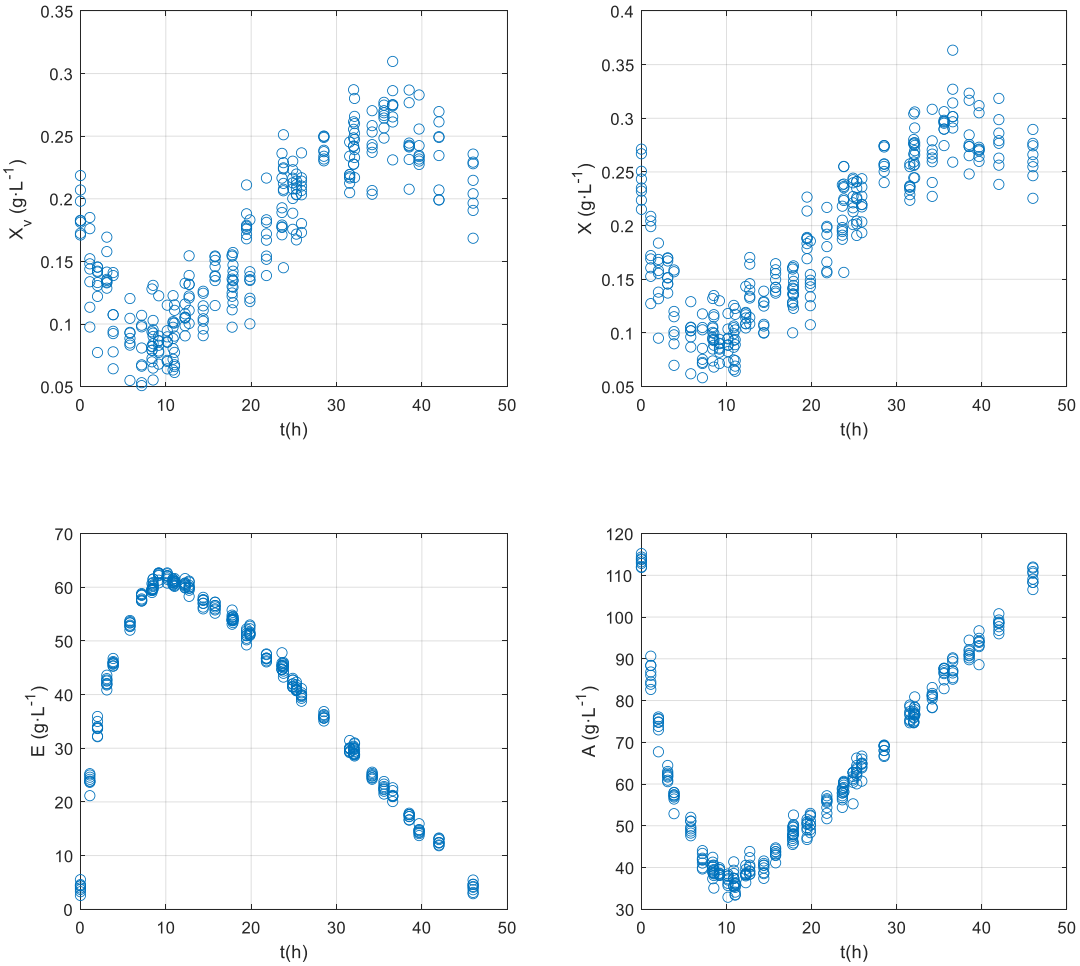

Figure S9. Time courses of the concentrations of the main variables from Experiment 6 (ten cycles)

Figure S10 shows viable cell (X_V), total cell (X), ethanol (E) and acetic acid (A) concentrations from ten cycles of Experiment 7, in which a continuous loading mode is used with E_{unload} = 3.5 % (v/v) (27.1 g·L^{-1}), $V_{unloaded}$ = 25 % and F_i = 0.06 L·min^{-1}.

Summary of main results:

- Mean ethanol uptake rate: 1.8±0.2 g·L^{-1}·h^{-1}.
- Acetic acid production rate: 17.8±0.3 g·h^{-1}.
- Length of loading phase: 0.6±0.1 h.
- Total length of cycle: 9.1±0.1 h.
- Maximum ethanol concentration reached at the end of loading phase: 42.6±0.8 g·L^{-1}.
- Maximum acetic acid concentration at the end of the cycle: 81±1 g·L^{-1}.

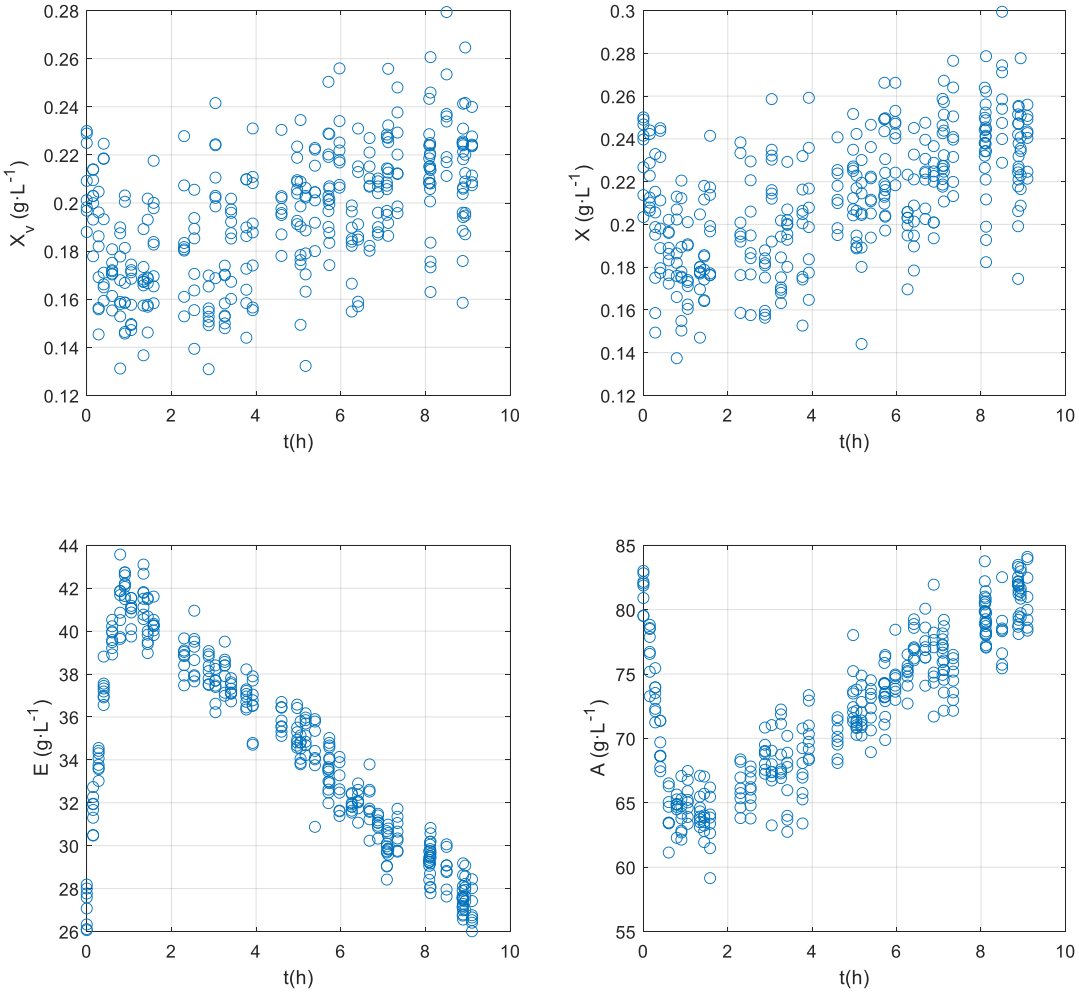

Figure S10. Time courses of the concentrations of the main variables from Experiment 7 (ten cycles)

Figure S11 shows viable cell (X_V), total cell (X), ethanol (E) and acetic acid (A) concentrations from ten cycles of Experiment 8, in which a semi-continuous ethanol-controlled loading mode is used with E_{unload} = 1.5 % (v/v) (11.6 g·L^{-1}), $V_{unloaded}$ = 50 %, E_{max} = 5 % (v/v) (38.8 g·L^{-1}) and F_i = 0.02 L·min^{-1}.

Summary of main results:

- Mean ethanol uptake rate: 1.6±0.2 g·L^{-1}·h^{-1}.
- Acetic acid production rate: 14.8±0.4 g·h^{-1}.
- Length of loading phase: 2.1±0.1 h.
- Total length of cycle: 8.3±0.7 h.
- Maximum ethanol concentration reached at the end of loading phase: 27.3±0.4 g·L^{-1}.
- Maximum acetic acid concentration at the end of the cycle: 101±2 g·L^{-1}.

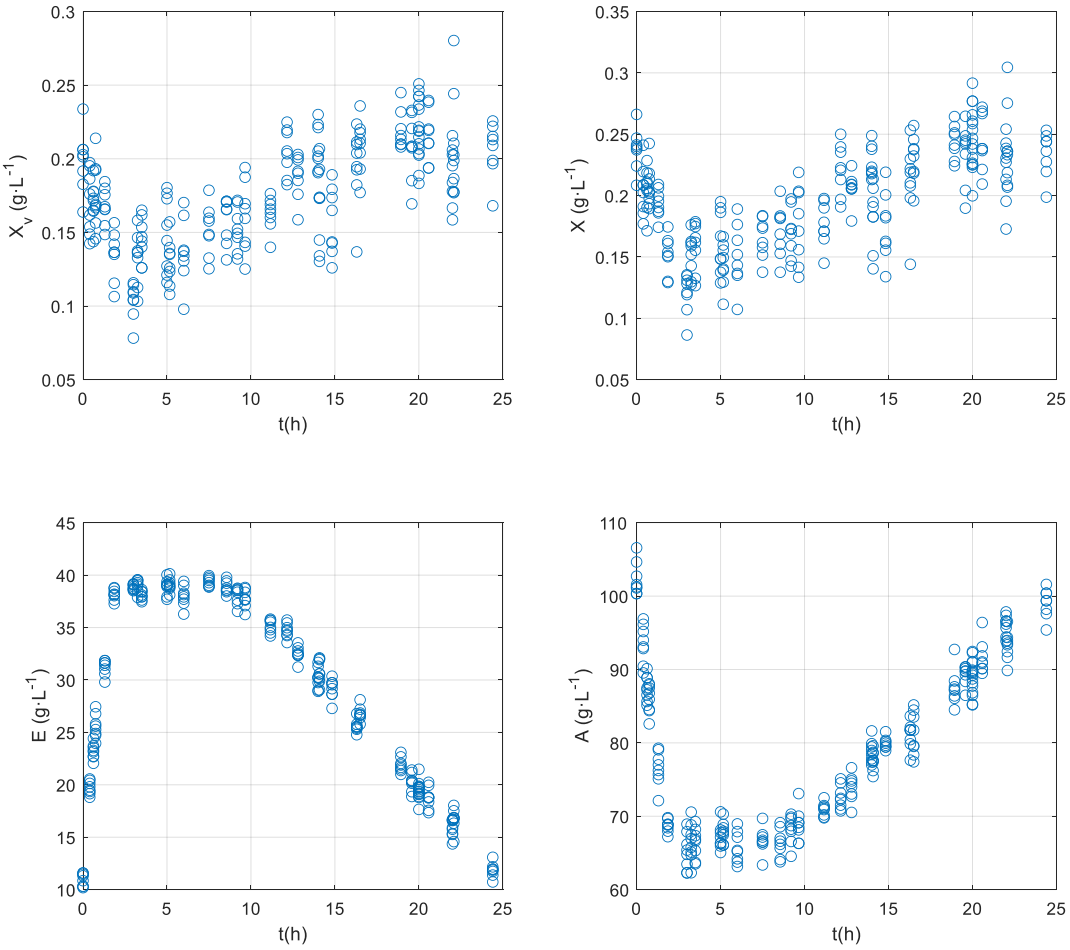

Figure S11. Time courses of the concentrations of the main variables from Experiment 8 (ten cycles)

Figure S12 shows viable cell (X_V), total cell (X), ethanol (E) and acetic acid (A) concentrations from ten cycles of Experiment 9, in which a semi-continuous ethanol-controlled loading mode is used with E_{unload} = 0.5 % (v/v) (3.9 g·L^{-1}), $V_{unloaded}$ = 50 %, E_{max} = 5 % (v/v) (38.8 g·L^{-1}) and F_i = 0.02 L·min^{-1}.

Summary of main results:

- Mean ethanol uptake rate: 1.5±0.1 g·L^{-1}·h^{-1}.
- Acetic acid production rate: 13.8±0.4 g·h^{-1}.
- Length of loading phase: 2.5±0.1 h.
- Total length of cycle: 6.8±0.4 h.
- Maximum ethanol concentration reached at the end of loading phase: 31.9±0.8 g·L^{-1}.
- Maximum acetic acid concentration at the end of the cycle: 110±2 g·L^{-1}.

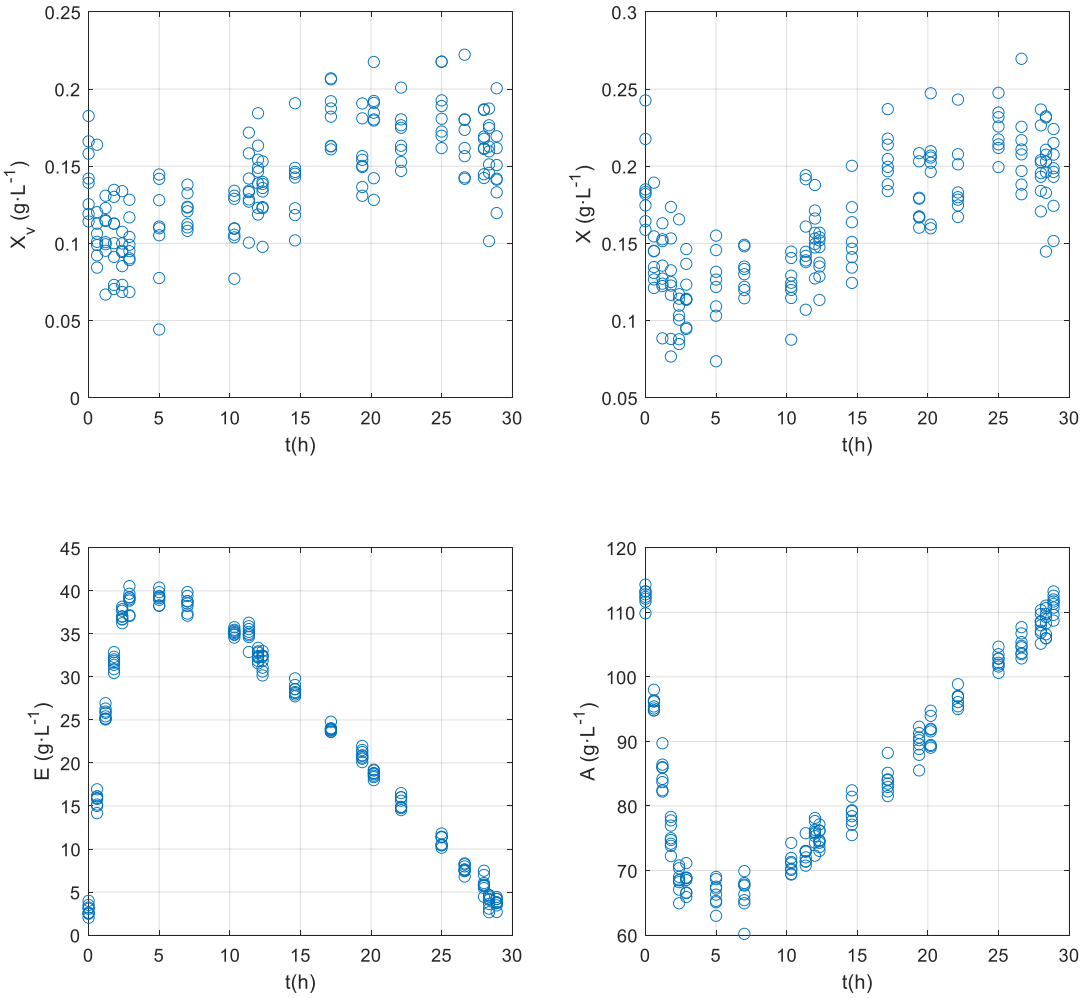

Figure S12. Time courses of the concentrations of the main variables from Experiment 9 (ten cycles)

S3. Simplified model simulation results

In this section, the considered model outputs (viable cell, non-viable cell, ethanol and acetic acid concentrations) from the simplified model, the initial model and the corresponding experimental data are shown in Figures S13-S21 for all the analysed experimental conditions (Table 1 in the main manuscript).

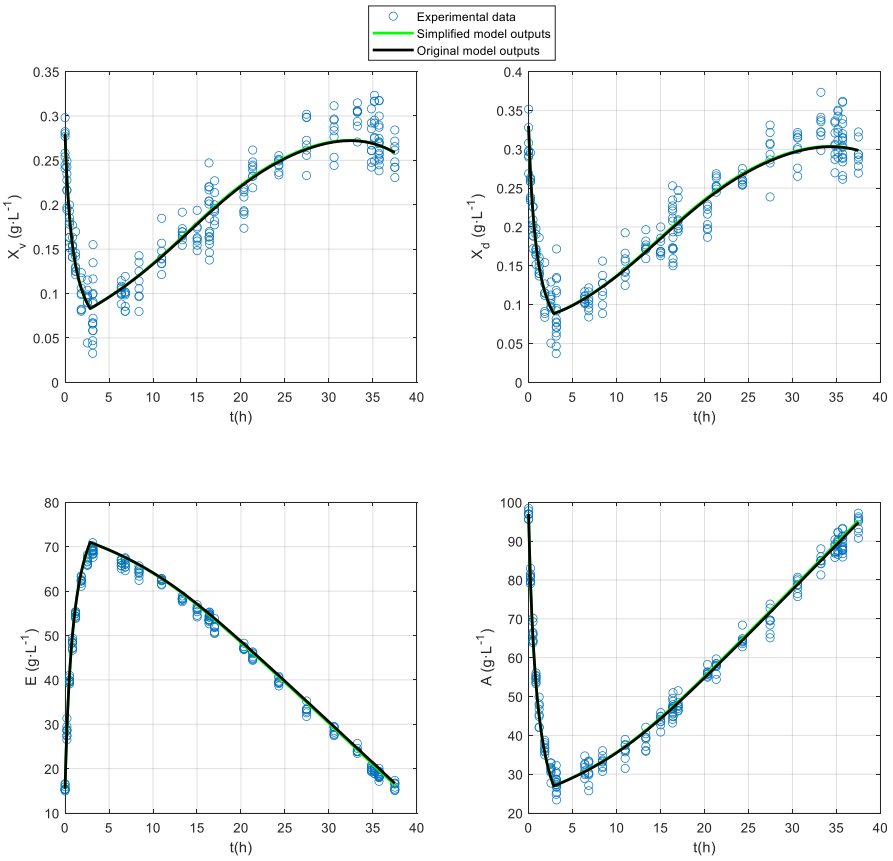

Figure S13. Simulation of outputs from initial and simplified models (Experiment 1)

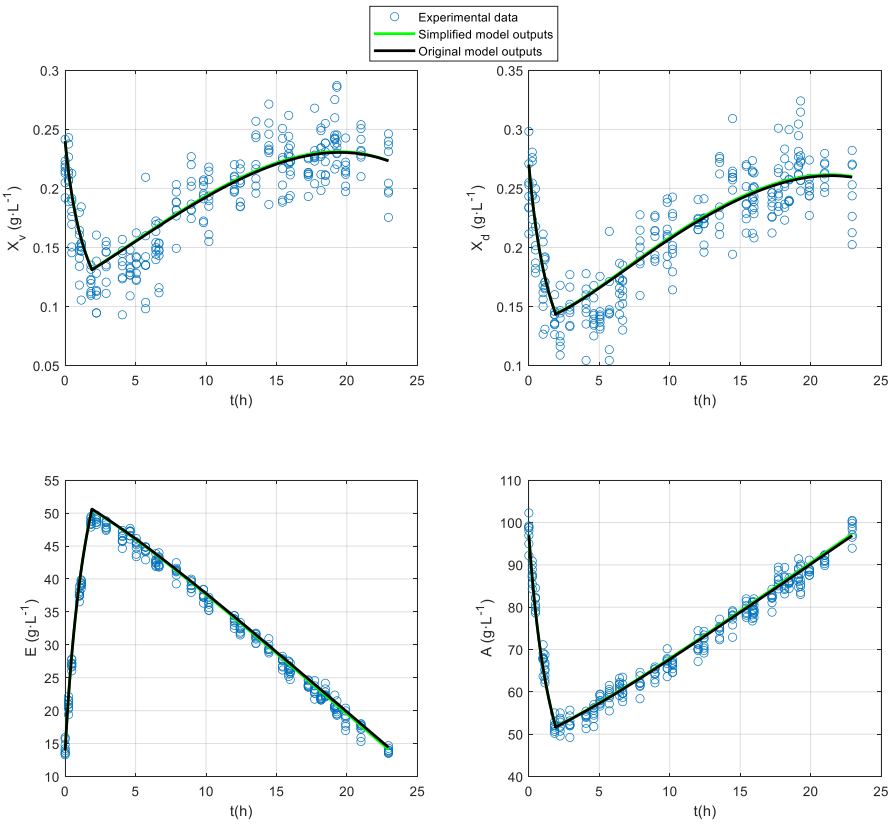

Figure S14. Simulation of outputs from initial and simplified models (Experiment 2)

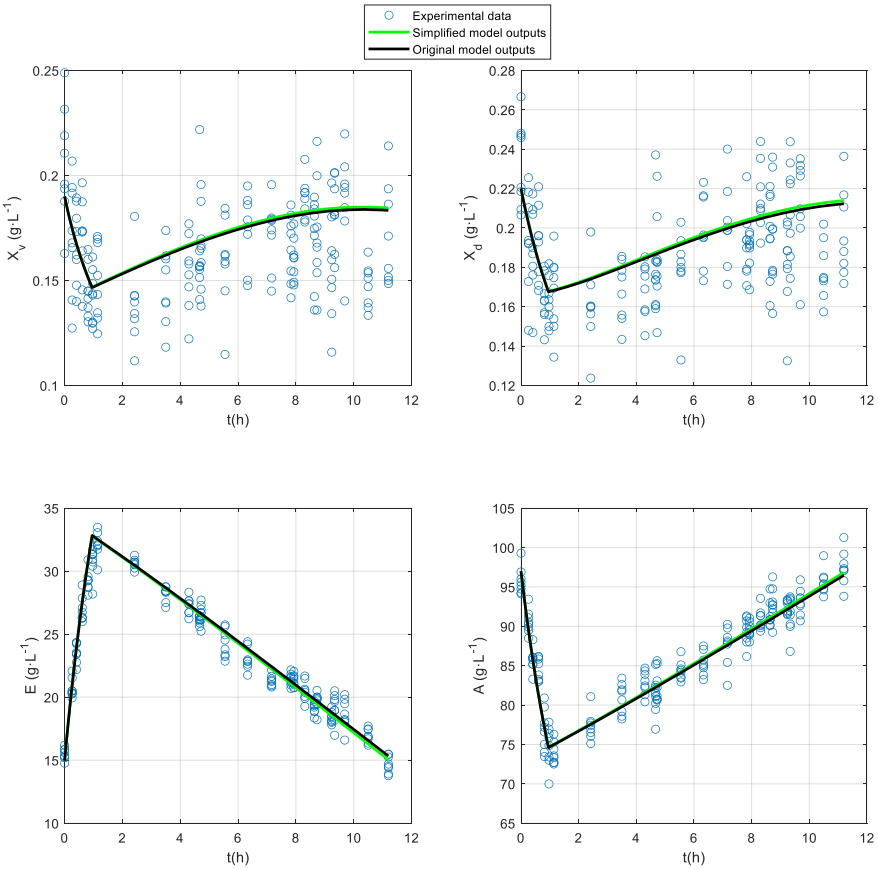

Figure S15. Simulation of outputs from initial and simplified models (Experiment 3)

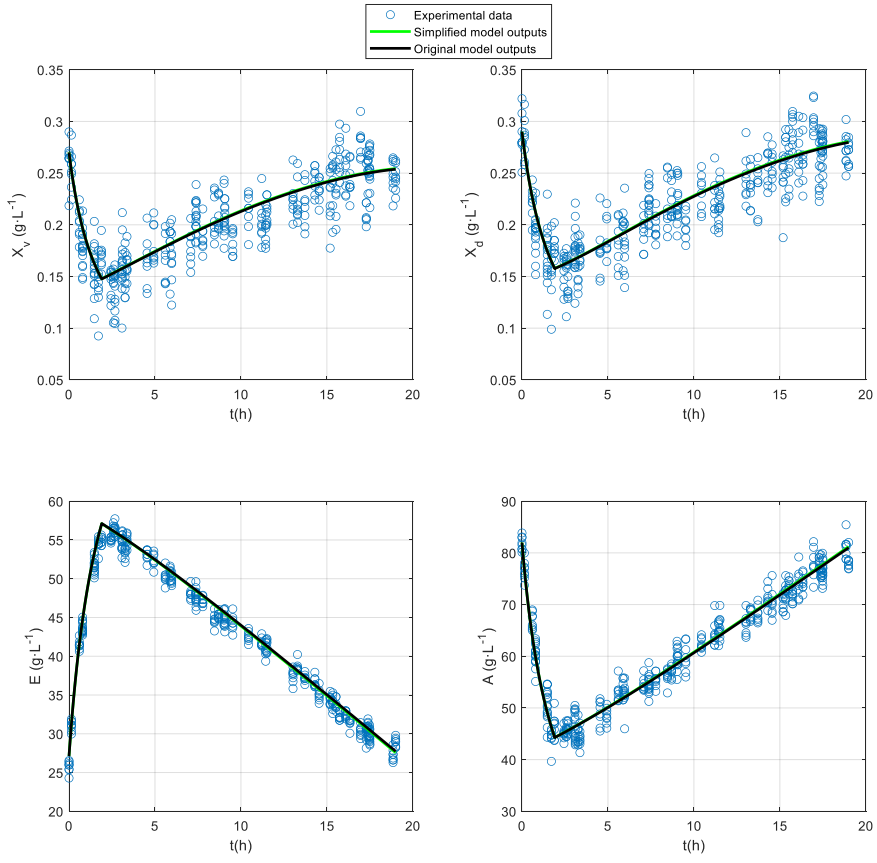

Figure S16. Simulation of outputs from initial and simplified models (Experiment 4)

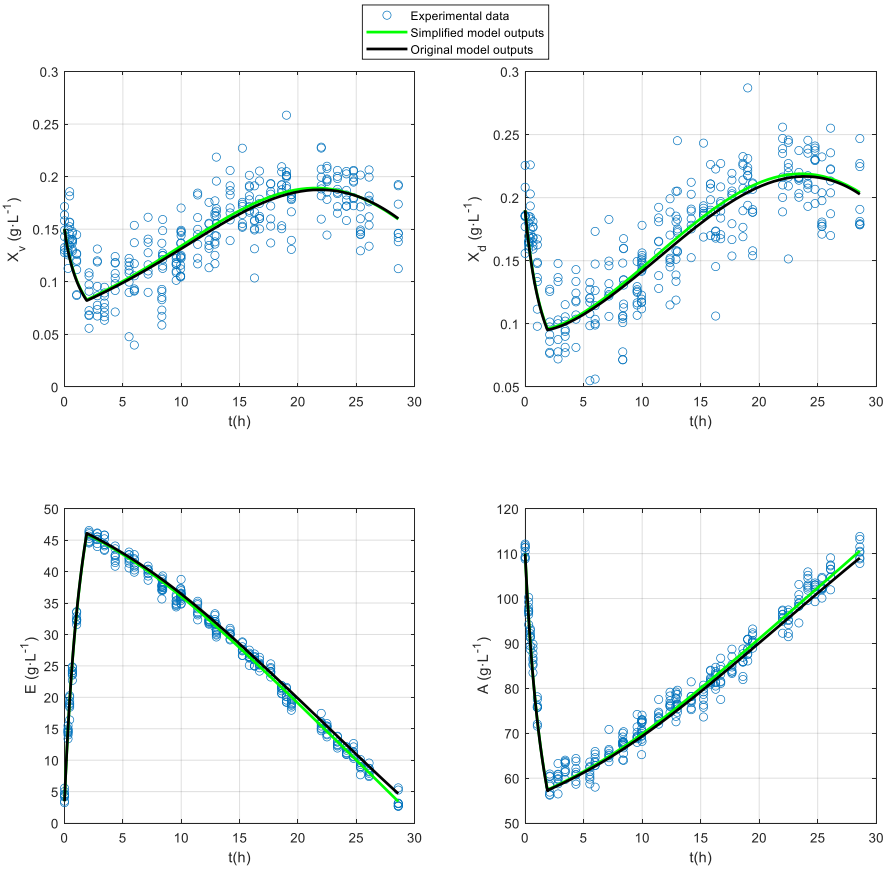

Figure S17. Simulation of outputs from initial and simplified models (Experiment 5)

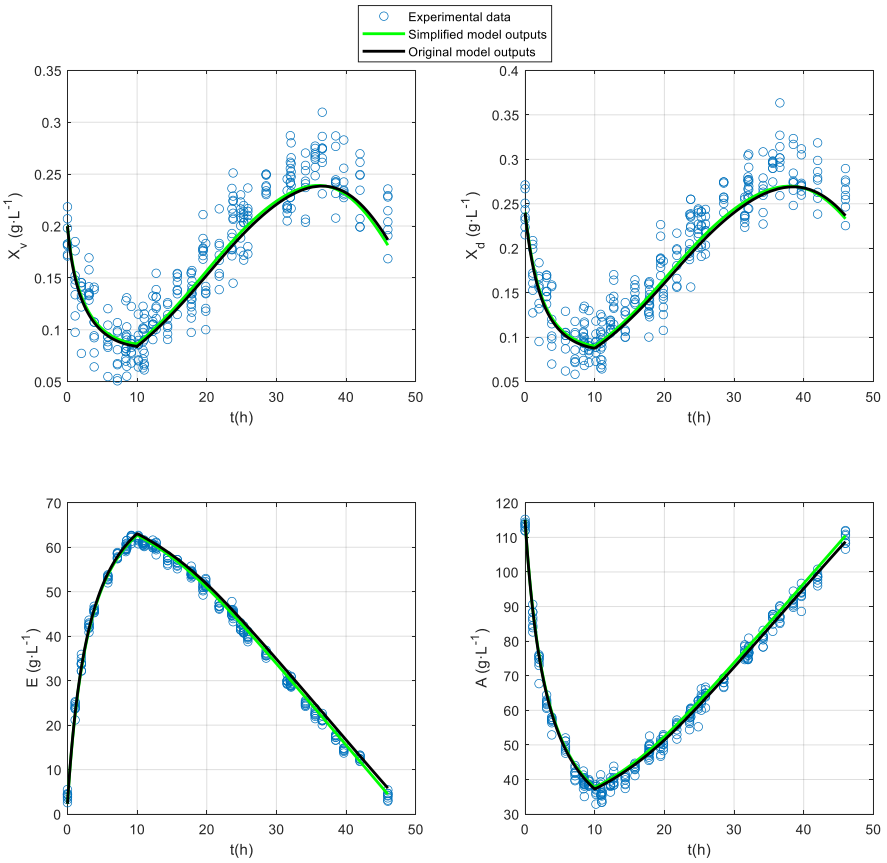

Figure S18. Simulation of outputs from initial and simplified models (Experiment 6)

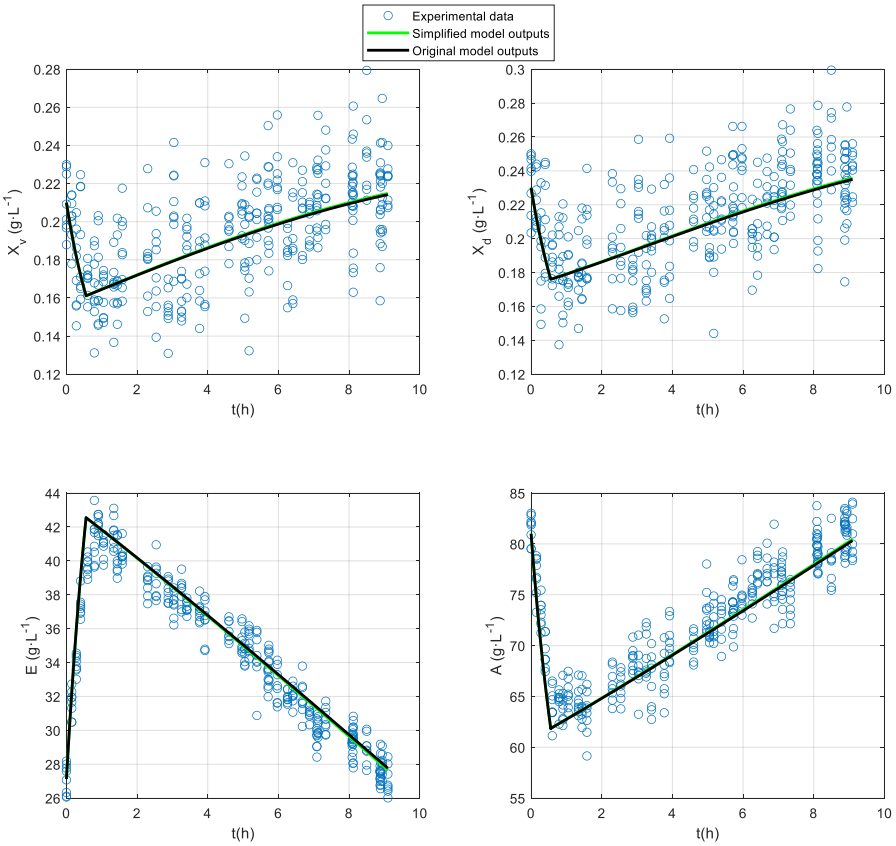

Figure S19. Simulation of outputs from initial and simplified models (Experiment 7)

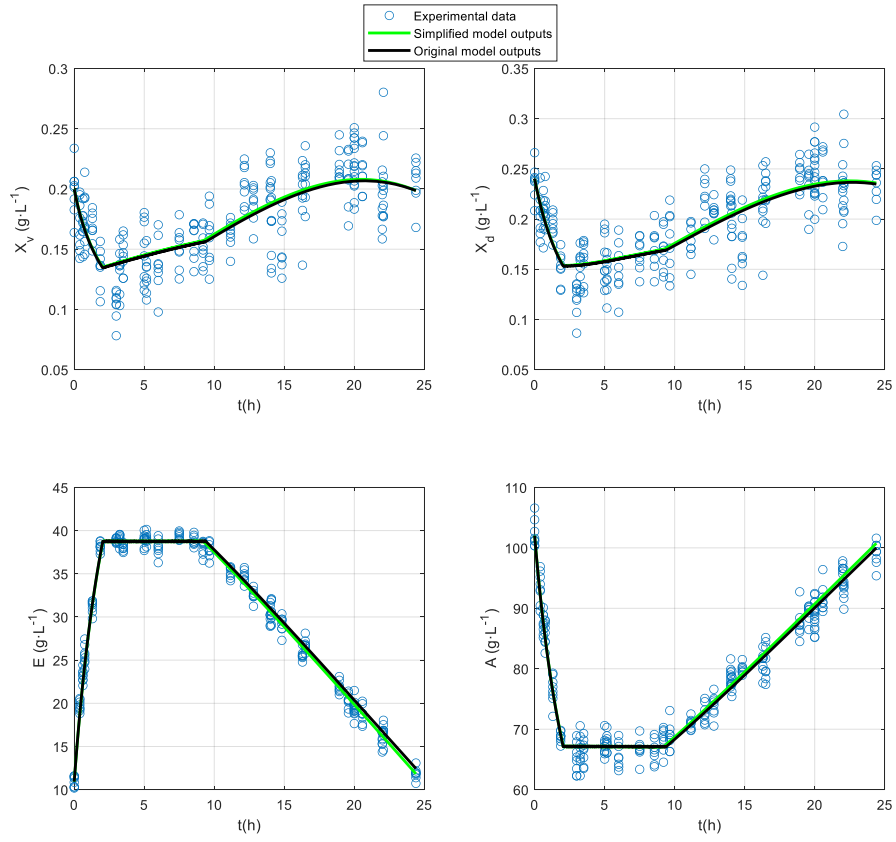

Figure S20. Simulation of outputs from initial and simplified models (Experiment 8)

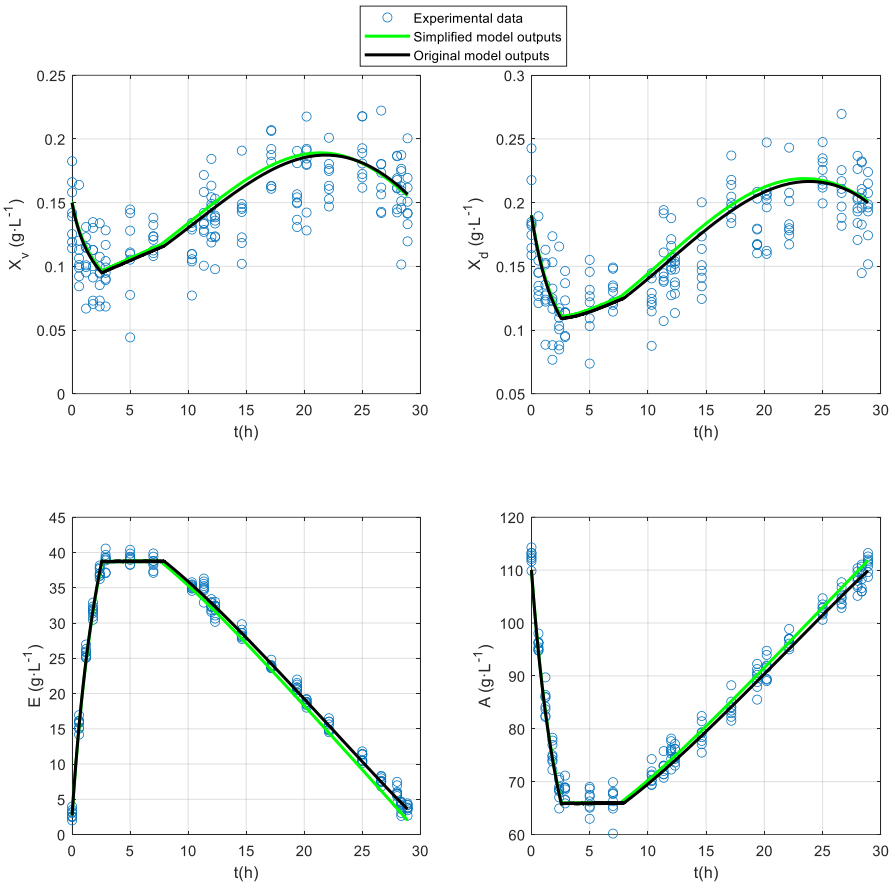

Figure S21. Simulation of outputs from initial and simplified models (Experiment 9)

Figure 1

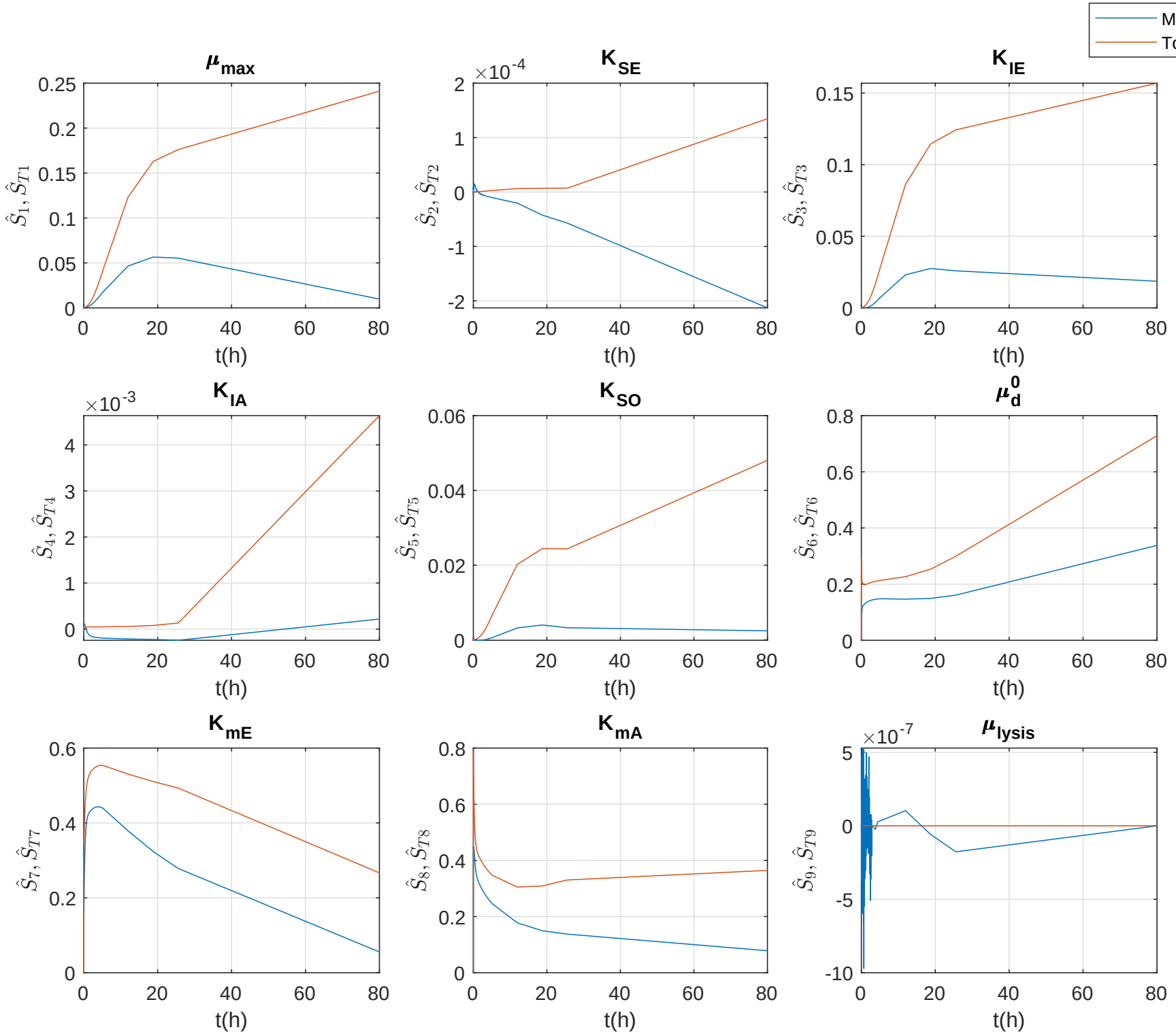
Main effects
Total effects
μ_{max}
K_{SE}
K_{IE}
K_{IA}
K_{SO}
μ_d^0
K_{mE}
K_{mA}
μ_{lysis}
$\hat{S}_1, \hat{S}_{T1}$
$\hat{S}_2, \hat{S}_{T2}$
$\hat{S}_3, \hat{S}_{T3}$
$\hat{S}_4, \hat{S}_{T4}$
$\hat{S}_5, \hat{S}_{T5}$
$\hat{S}_6, \hat{S}_{T6}$
$\hat{S}_7, \hat{S}_{T7}$
$\hat{S}_8, \hat{S}_{T8}$
$\hat{S}_9, \hat{S}_{T9}$
$\times 10^{-4}$
$\times 10^{-3}$
$\times 10^{-7}$
t(h)

Figure 2

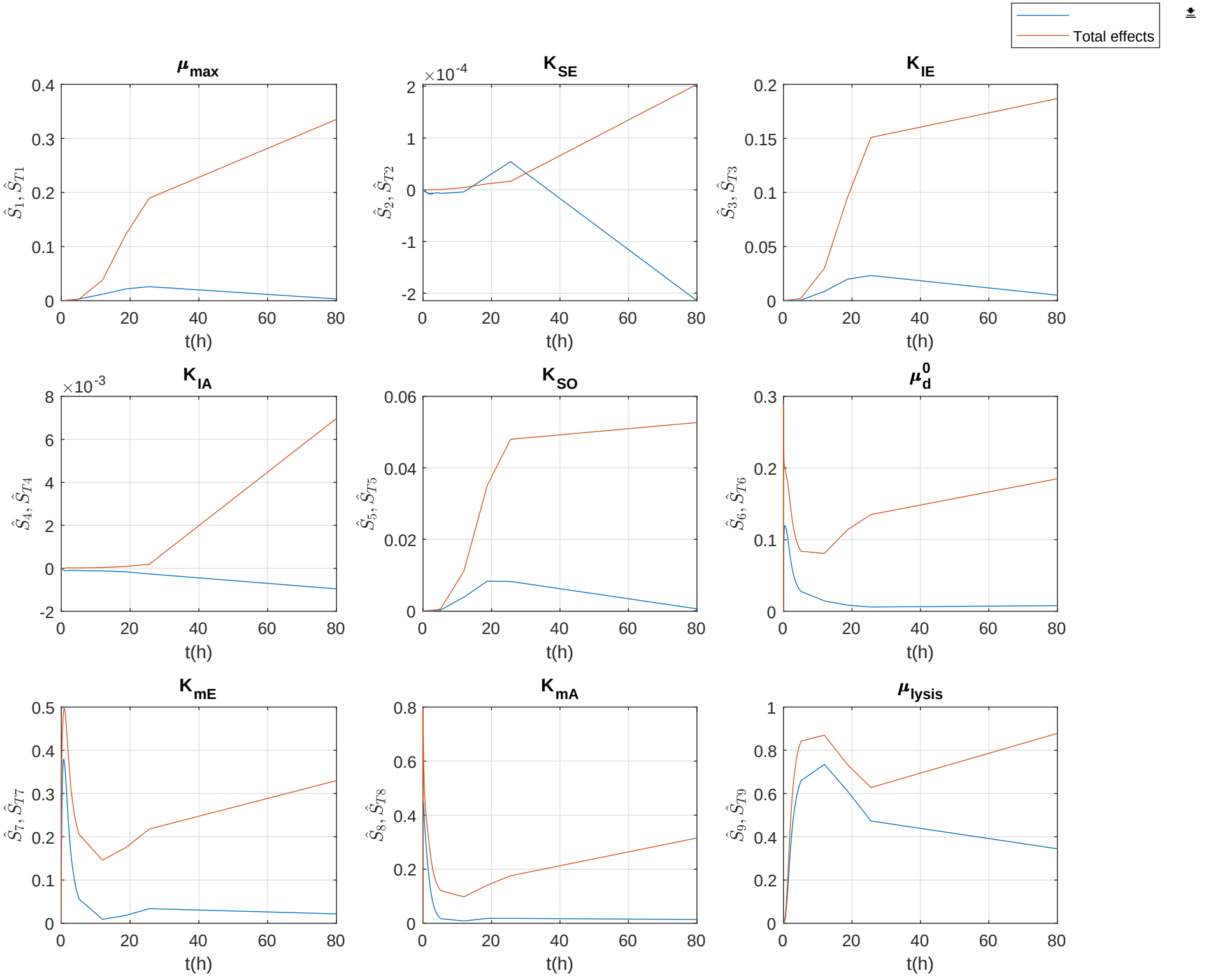
Total effects
μ_{max}
K_{SE}
K_{IE}
K_{IA}
K_{SO}
μ_d^0
K_{mE}
K_{mA}
μ_{lysis}
$\hat{S}_1, \hat{S}_{T1}$
$\hat{S}_2, \hat{S}_{T2}$
$\hat{S}_3, \hat{S}_{T3}$
$\hat{S}_4, \hat{S}_{T4}$
$\hat{S}_5, \hat{S}_{T5}$
$\hat{S}_6, \hat{S}_{T6}$
$\hat{S}_7, \hat{S}_{T7}$
$\hat{S}_8, \hat{S}_{T8}$
$\hat{S}_9, \hat{S}_{T9}$
$\times 10^{-4}$
$\times 10^{-3}$
t(h)

Figure 3

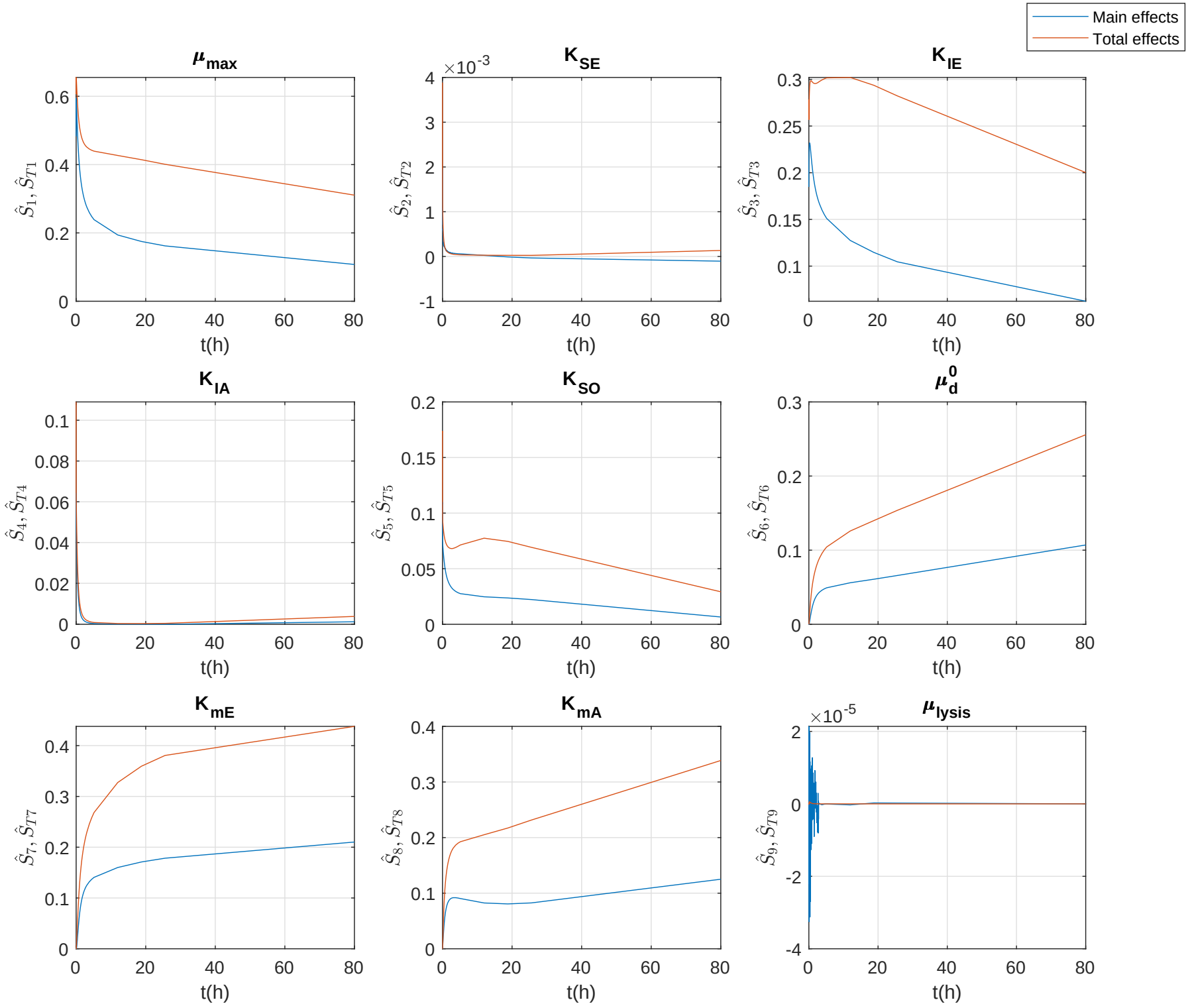
Main effects
Total effects
μ_{max}
K_{SE}
K_{IE}
K_{IA}
K_{SO}
μ_d^0
K_{mE}
K_{mA}
μ_{lysis}
$\times 10^{-3}$
$\times 10^{-5}$
$\hat{S}_1, \hat{S}_{T1}$
$\hat{S}_2, \hat{S}_{T2}$
$\hat{S}_3, \hat{S}_{T3}$
$\hat{S}_4, \hat{S}_{T4}$
$\hat{S}_5, \hat{S}_{T5}$
$\hat{S}_6, \hat{S}_{T6}$
$\hat{S}_7, \hat{S}_{T7}$
$\hat{S}_8, \hat{S}_{T8}$
$\hat{S}_9, \hat{S}_{T9}$
t(h)

Figure 4

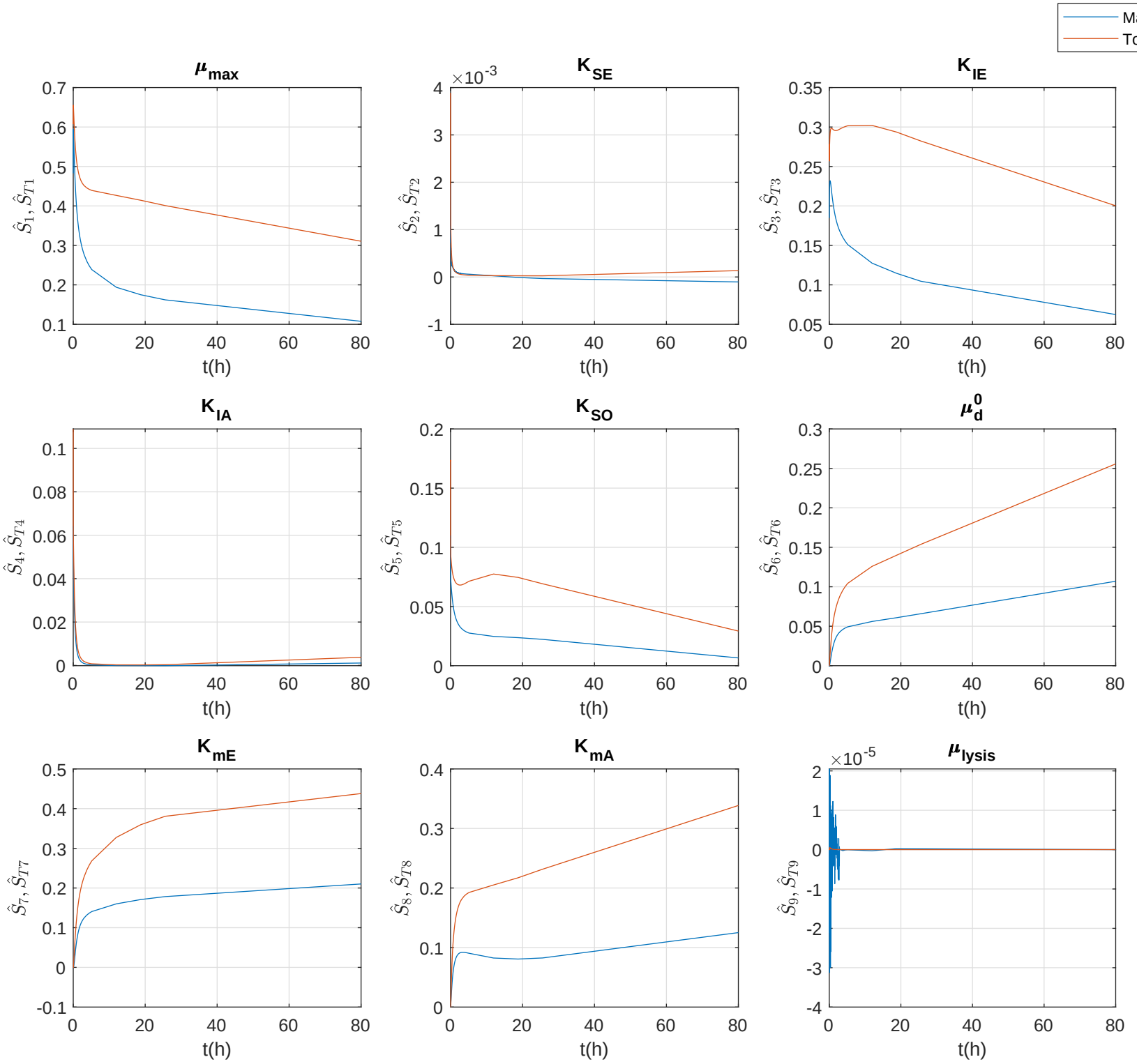
Main effects
Total effects
μ_{max}
K_{SE}
K_{IE}
K_{IA}
K_{SO}
μ_d^0
K_{mE}
K_{mA}
μ_{lysis}
$\times 10^{-3}$
$\times 10^{-5}$
$\hat{S}_1, \hat{S}_{T1}$
$\hat{S}_2, \hat{S}_{T2}$
$\hat{S}_3, \hat{S}_{T3}$
$\hat{S}_4, \hat{S}_{T4}$
$\hat{S}_5, \hat{S}_{T5}$
$\hat{S}_6, \hat{S}_{T6}$
$\hat{S}_7, \hat{S}_{T7}$
$\hat{S}_8, \hat{S}_{T8}$
$\hat{S}_9, \hat{S}_{T9}$
t(h)

Figure 5

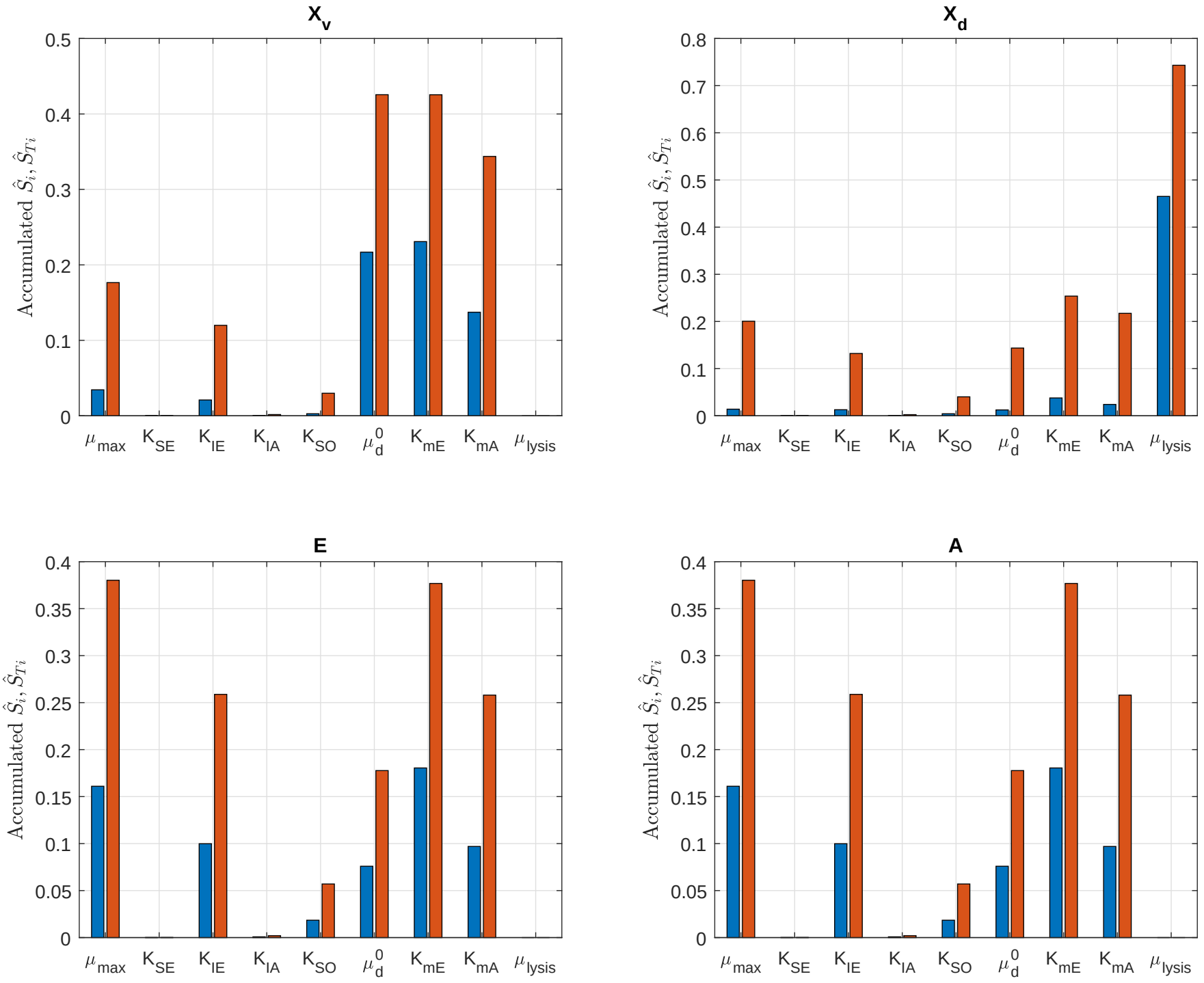
X_v
X_d
E
A
Accumulated $\hat{S}_i, \hat{S}_{Ti}$
μ_{max}
K_{SE}
K_{IE}
K_{IA}
K_{SO}
μ_d^0
K_{mE}
K_{mA}
μ_{lysis}

Figure 6

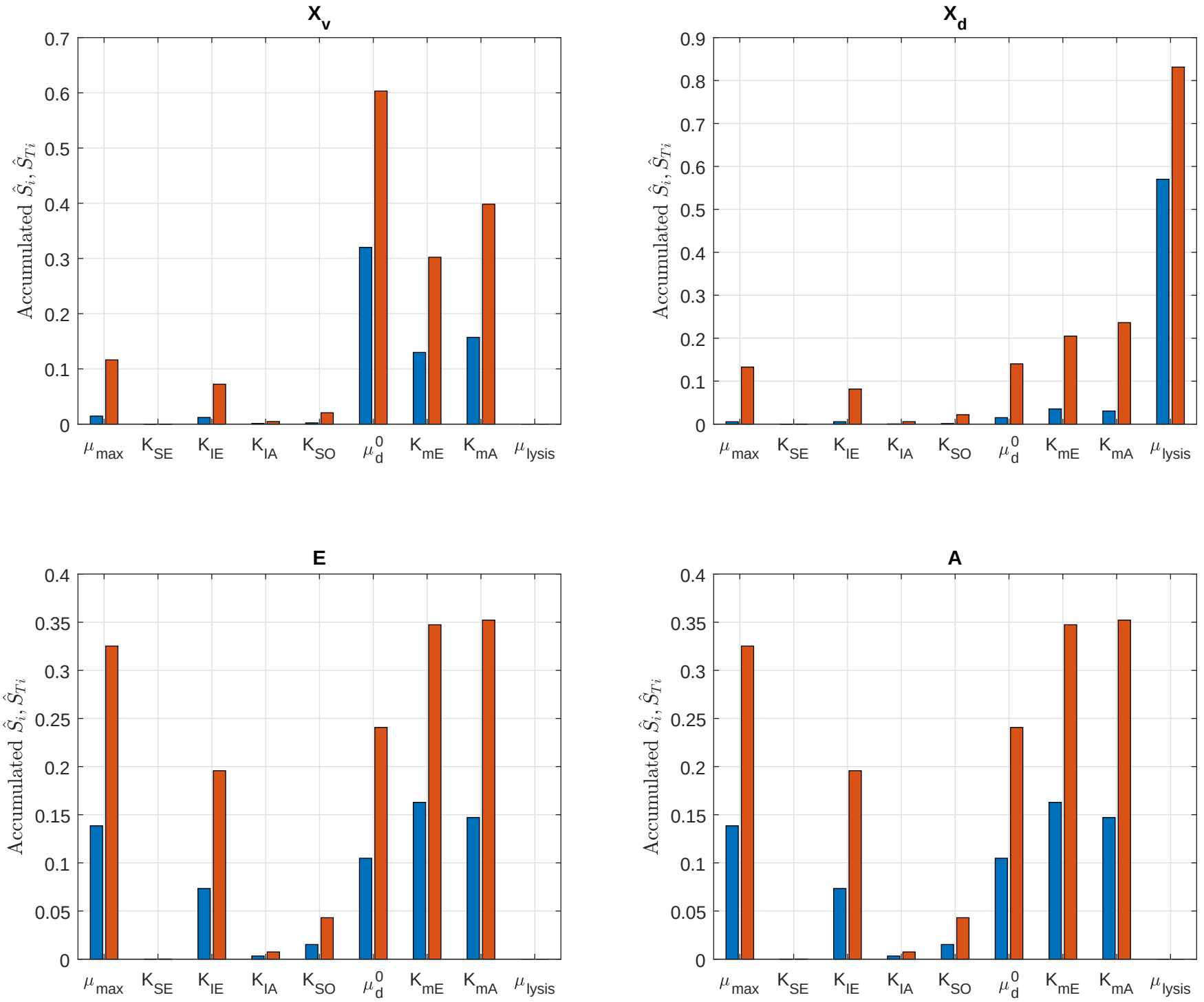
X_v
X_d
E
A
Accumulated $\hat{S}_i, \hat{S}_{Ti}$
μ_{max}
K_{SE}
K_{IE}
K_{IA}
K_{SO}
μ_d^0
K_{mE}
K_{mA}
μ_{lysis}

Figure 7

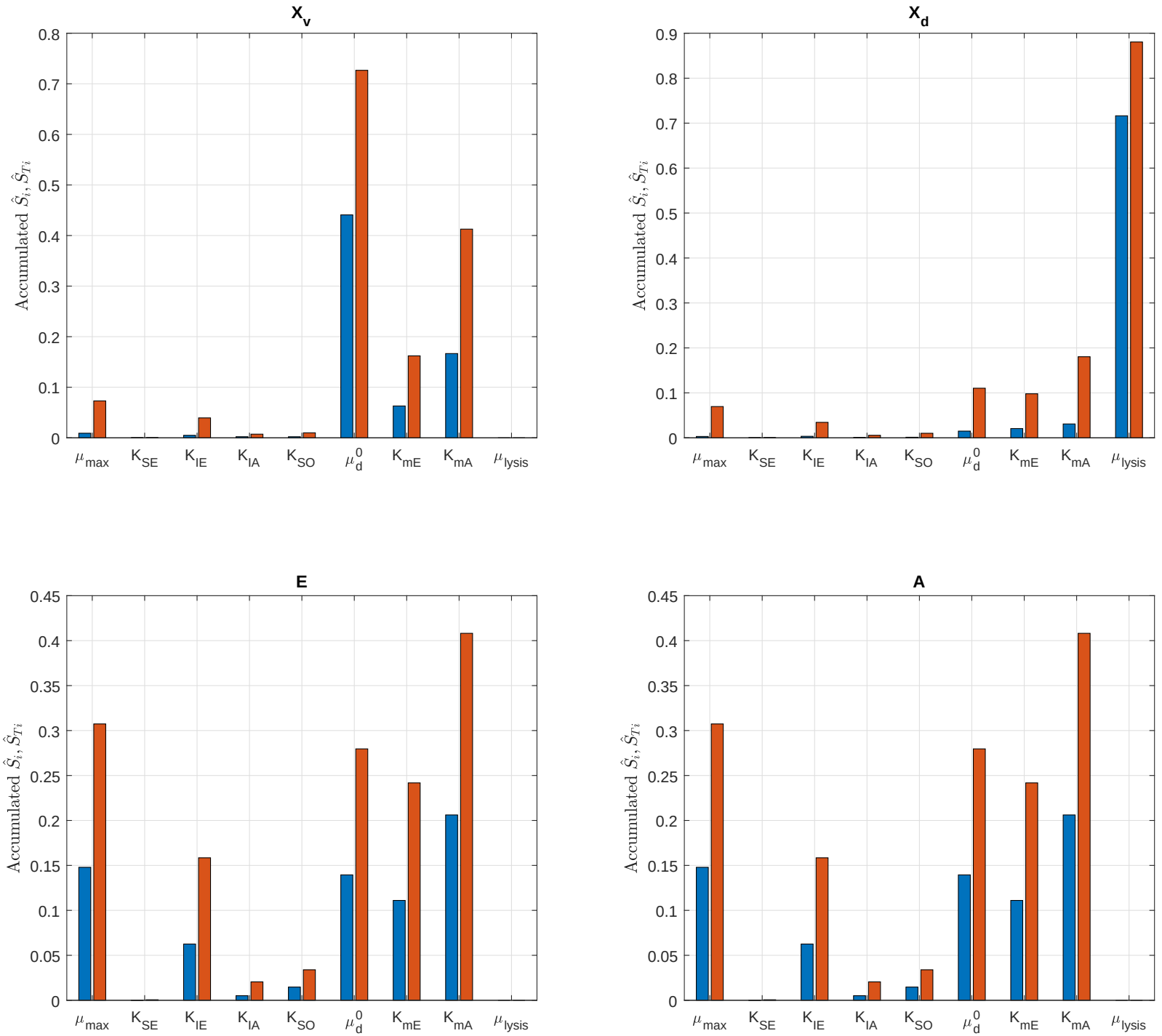
X_v
X_d
E
A
Accumulated $\hat{S}_i, \hat{S}_{Ti}$
μ_{max}
K_{SE}
K_{IE}
K_{IA}
K_{SO}
μ_d^0
K_{mE}
K_{mA}
μ_{lysis}

Figure 8

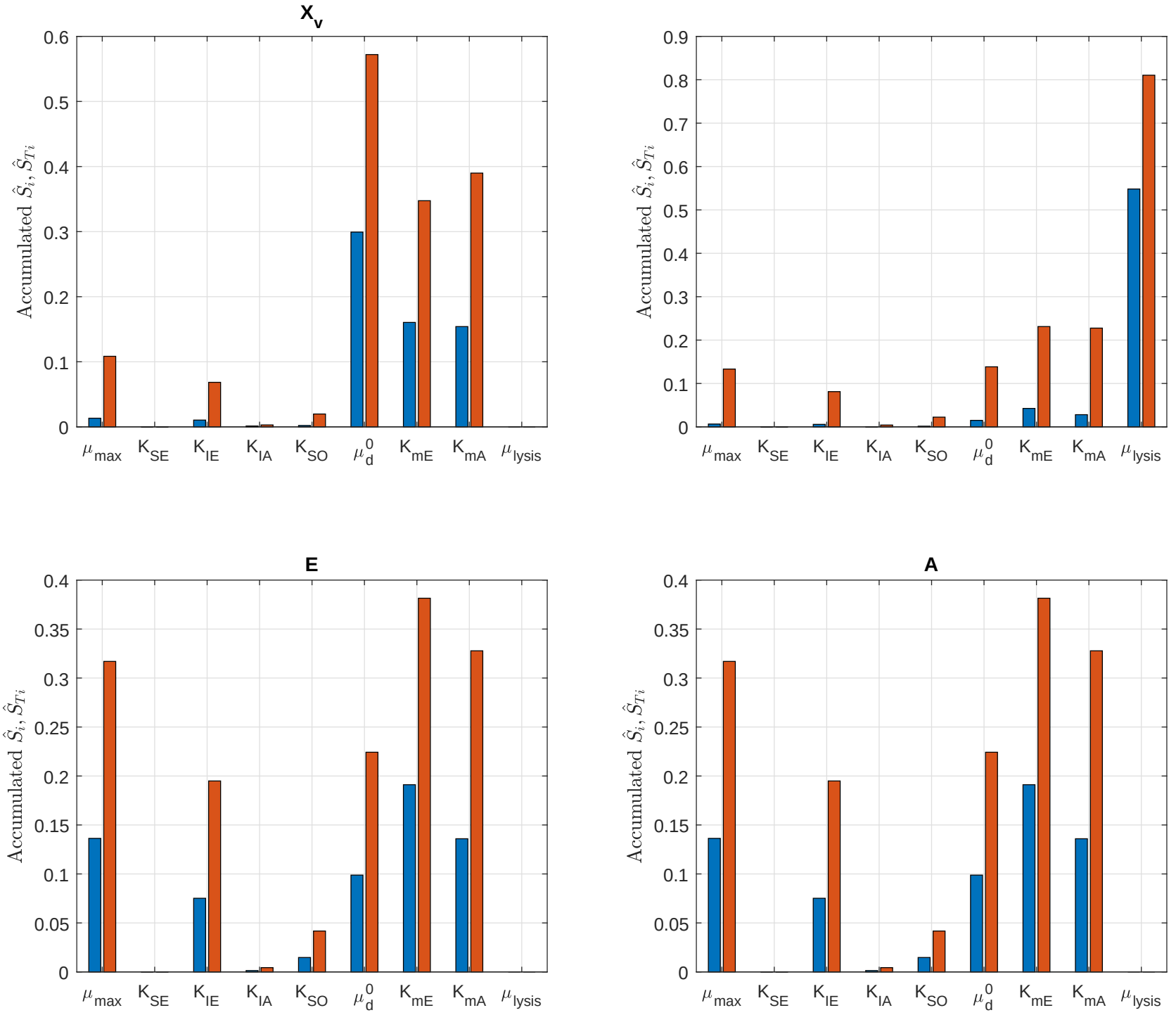
X_v
E
A
Accumulated $\hat{S}_i, \hat{S}_{Ti}$
μ_{max}
K_{SE}
K_{IE}
K_{IA}
K_{SO}
μ_d^0
K_{mE}
K_{mA}
μ_{lysis}

Figure 9

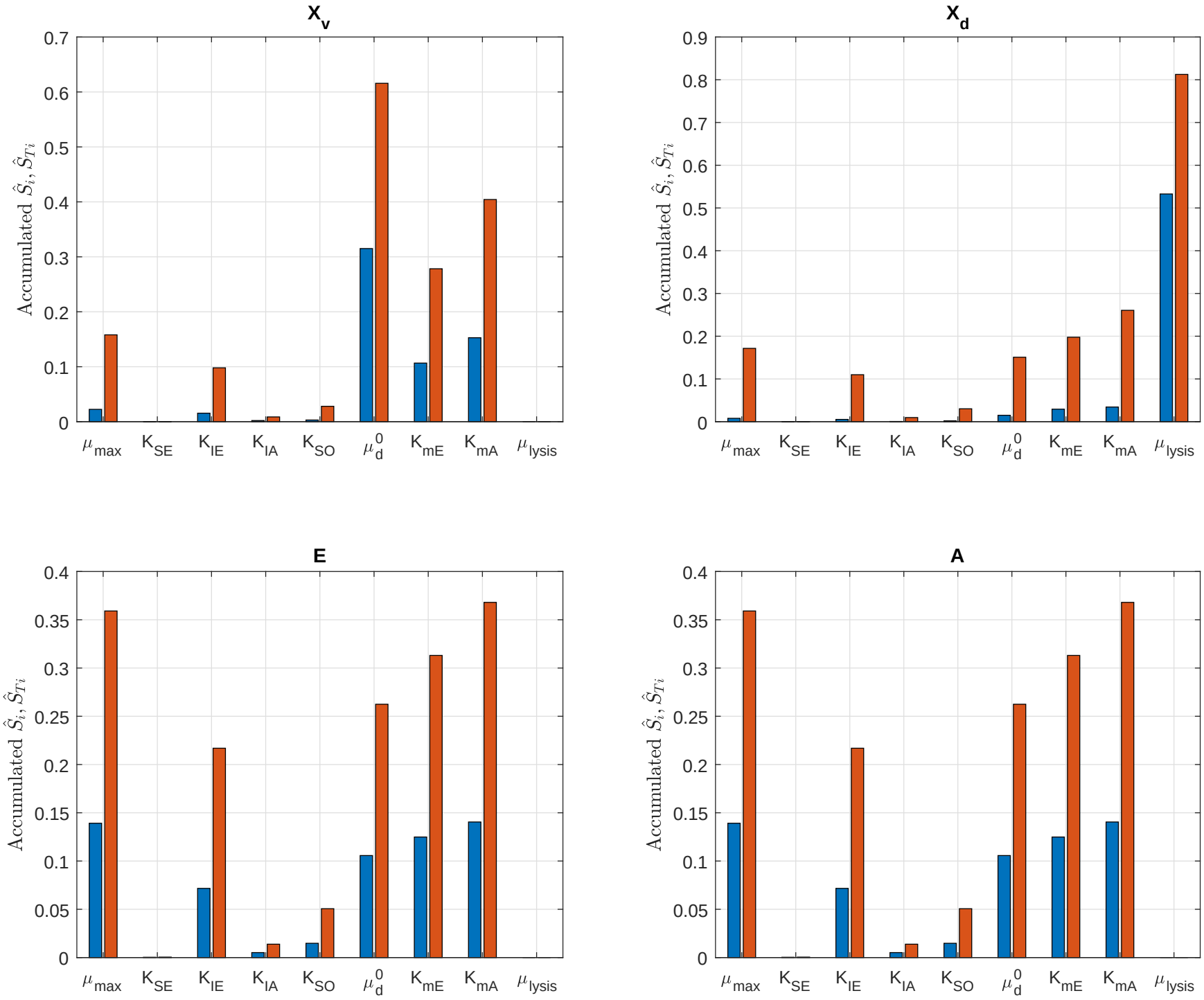
X_v
X_d
E
A
Accumulated $\hat{S}_i, \hat{S}_{Ti}$
μ_{max}
K_{SE}
K_{IE}
K_{IA}
K_{SO}
μ_d^0
K_{mE}
K_{mA}
μ_{lysis}

Figure 10

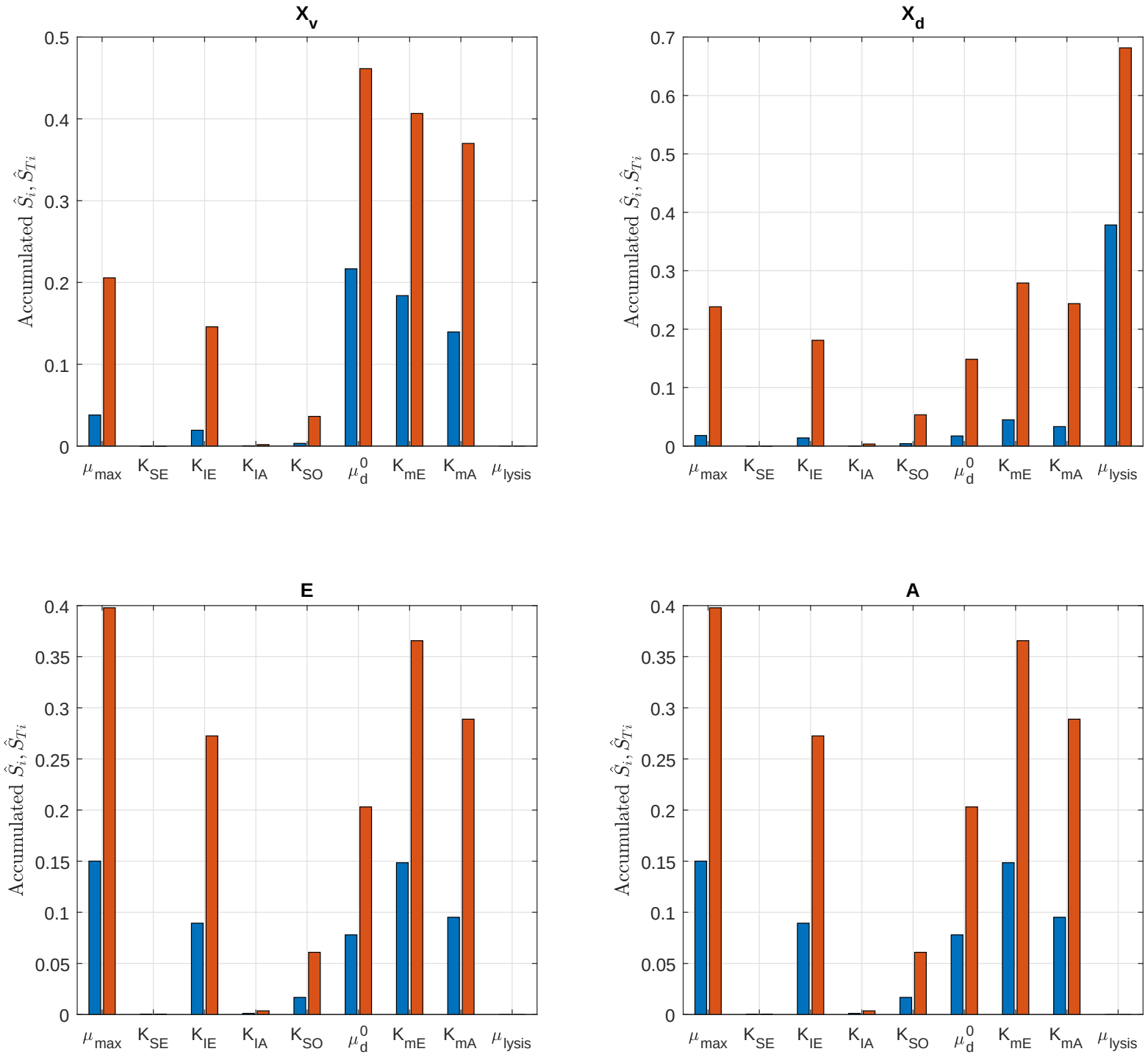
X_v
X_d
E
A
Accumulated $\hat{S}_i, \hat{S}_{Ti}$
μ_{max}
K_{SE}
K_{IE}
K_{IA}
K_{SO}
μ_d^0
K_{mE}
K_{mA}
μ_{lysis}

Figure 11

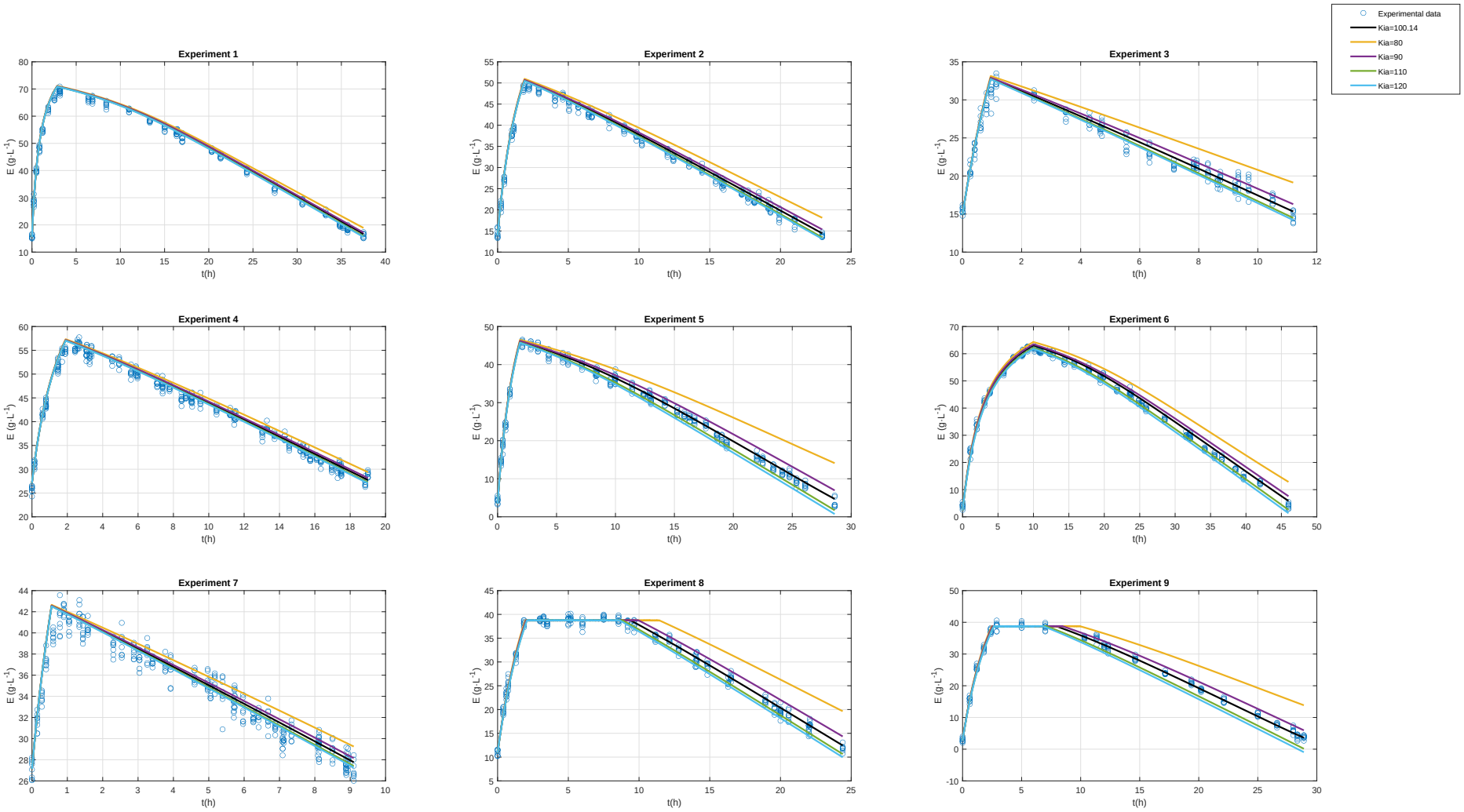
Experimental data
Kia=100.14
Kia=80
Kia=90
Kia=110
Kia=120
Experiment 1
Experiment 2
Experiment 3
Experiment 4
Experiment 5
Experiment 6
Experiment 7
Experiment 8
Experiment 9
E (g·L-1)
t(h)

Figure 12

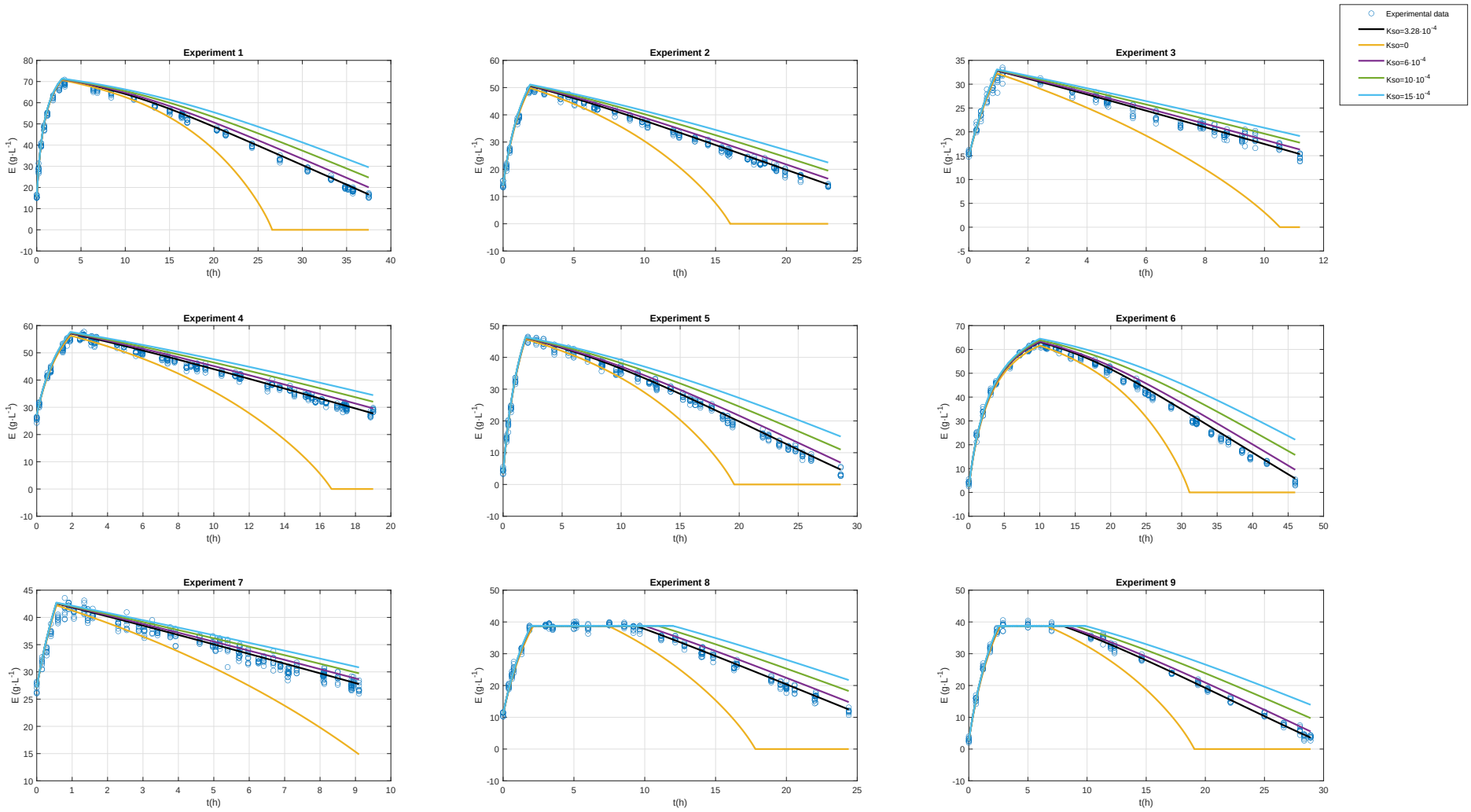
Experiment 1
Experiment 2
Experiment 3
Experiment 4
Experiment 5
Experiment 6
Experiment 7
Experiment 8
Experiment 9
E (g·L-1)
t(h)
Experimental data
Kso=3.28·10-4
Kso=0
Kso=6·10-4
Kso=10·10-4
Kso=15·10-4

Figure 13

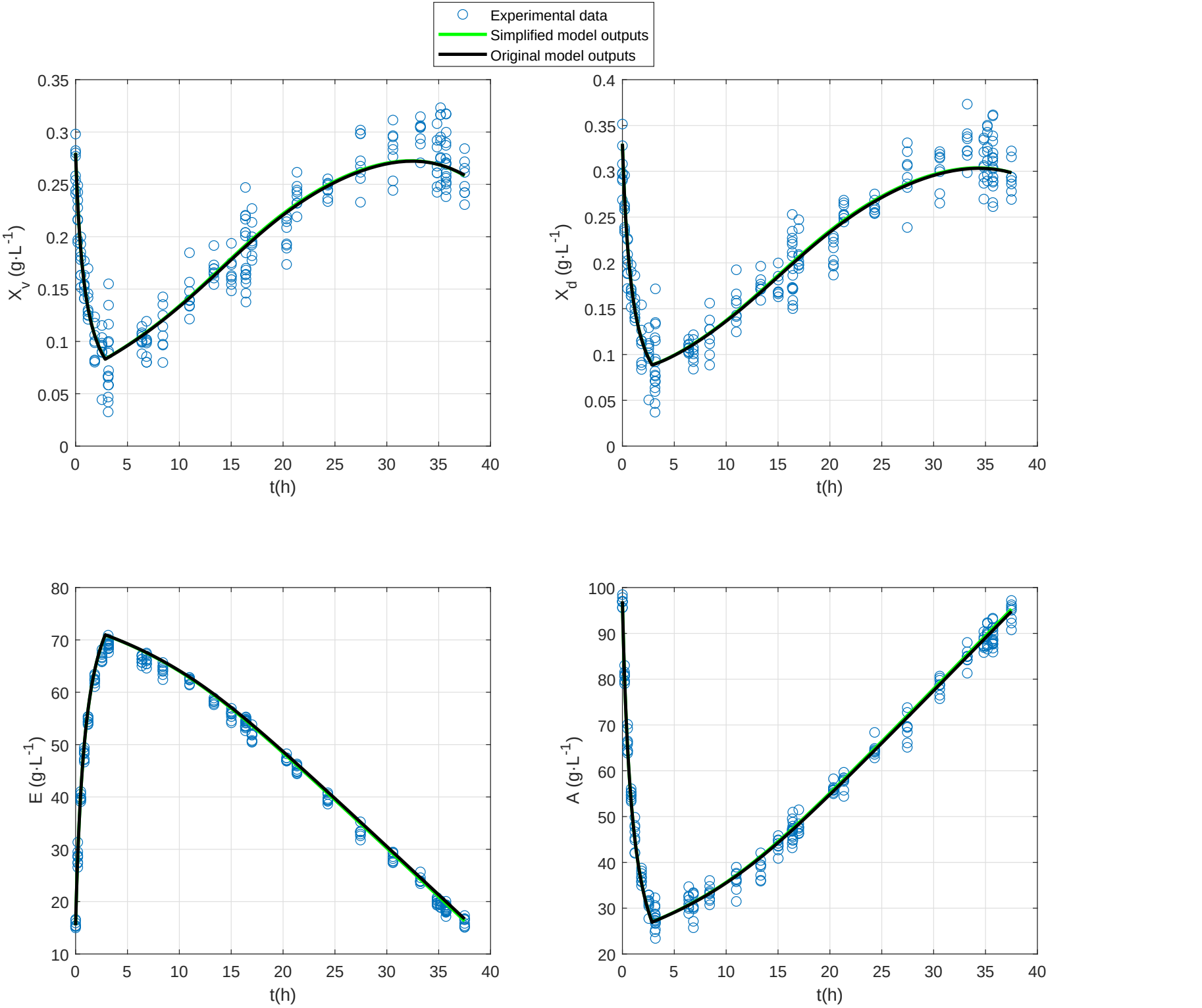
Experimental data
Simplified model outputs
Original model outputs
X_v (g·L^{-1})
X_d (g·L^{-1})
E (g·L^{-1})
A (g·L^{-1})
t(h)

Figure 14

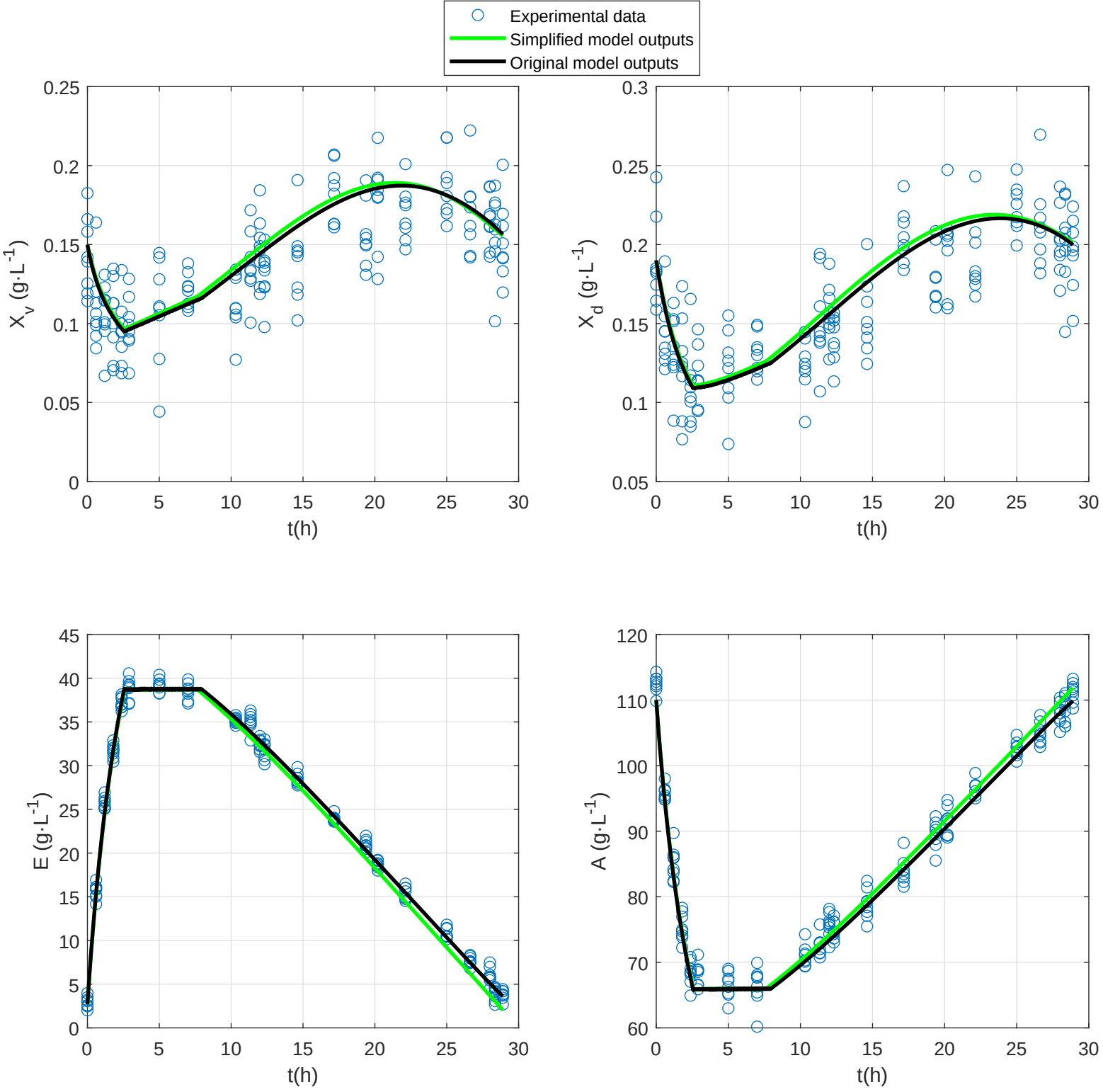
Experimental data
Simplified model outputs
Original model outputs
X_v (g·L^{-1})
X_d (g·L^{-1})
E (g·L^{-1})
A (g·L^{-1})
t(h)